



Manabu Shiraiwa  
Assistant Professor  
Department of Chemistry  
University of California, Irvine  
Irvine, CA 92697-2025, USA

Office. Tel: 949-824-5101  
Fax: 949-824-8571  
E-mail: m.shiraiwa@uci.edu

October 4, 2016

**Submission of revised manuscript: acp-2016-501**

Dear Prof. Kiendler-Scharr:

Please find attached a revised manuscript for the journal Atmospheric Chemistry and Physics: “Quantification of environmentally persistent free radicals and reactive oxygen species in atmospheric aerosol particles” by A. M. Arangio et al.

Four referee comments were very helpful in improving the manuscript. We have addressed and implemented practically all of the comments as detailed in the attached author’s response. Changes in the manuscript are highlighted in blue in the marked-up copy.

We are confident that the revised manuscript meets the quality standards of ACP. In view of the very positive referee comments and discussion published in ACPD, we look forward to positive response from you.

Thanks and best regards,

Manabu Shiraiwa

## **Response to the comment to the Anonymous Referee #1**

The paper from Arangio et al. measures the concentration of environmentally persistent free radicals (EPFR) and reactive oxygen species (ROS) in size segregated ambient aerosols. EPFR were measured directly by EPR spectrometer, while the ROS were measured by extracting the particles in water and then EPR analysis. As per the reviewer's knowledge, this is first comprehensive measurement of EPFR and ROS in size-segregated aerosols. ROS are an important species in ambient aerosols and could be biologically relevant. In addition to these novel measurements, authors also throw lights on the possible mechanisms of ROS generation through redox cycling between organic compounds and transition metals. An improved understanding of these mechanisms is important to comprehend the aging process of atmospheric aerosols. The paper is well written and easily comprehensible. Therefore, I recommend the publication of this manuscript. However, I have few comments which the authors should consider to make their work better:

### **Response:**

We thank the referee's review and very positive evaluation of this manuscript. The point-by point responses are given below.

Page 2, Line 42: Are there literature evidences that organic radicals also mediate in the oxidative stress? If yes, then authors should include them.

### **Response:**

Some types of organic radicals such as semiquinone and phenoxy radicals are known to play a role in oxidative stress (Pryor et al., 1995; Winterbourn, 2008; Birben et al., 2012). We have added new references.

Page 3, Line 87: Why these two samples were collected for a longer duration? Are the authors not concerned about the loss of semivolatiles during that long sampling duration?

### **Response:**

We agree that semi-volatile compounds may be lost for long sampling duration, which is a common problem of the particle collection using an impactor. Two samples were collected for 48 h in order to obtain sufficiently high mass loadings for all particle size ranges. We have clarified this point in the revised manuscript.

Page 4, Line 128: Authors should somewhere explain these units of spins  $\mu\text{g}^{-1}$ , probably in the method section.

Response:

The unit spins  $\mu\text{g}^{-1}$  indicates the number of spins (or radicals) per  $\mu\text{g}$  of particle mass. We will clarify it in the revised manuscript.

Page 4, Line 129-131: Can authors elaborate on their sentence that EPFR distribution is similar to soot? Do you mean that there is commonality in the sources of two?

Response:

Yes, we think that the sources of soot and EPFR are very similar (e.g., combustion) and EPFR may be often associated with soot particles (Dellinger et al., 2001). We will clarify this point in the revised manuscript.

Page 5, Line 143: Why the samples collected on these two days are significant and discussed separately?

Response:

As explained above, for certain periods we have collected particles for 48 h to collect enough particle mass to perform EPFR and ROS analysis for wide particle diameters (50 nm - 1.8  $\mu\text{m}$ ). On the other hand, particles collected for 13 days with a sampling time of 24h were focused on limited particle size range of 50 nm to 500 nm diameter particles.

Page 5, Line 143-150: I am not sure why the authors have discussed the sampling duration separately. The EPFR concentration expressed in units of spin/ $\mu\text{g}$  should not be affected by the sampling duration.

Response:

Indeed the EPFR concentrations are not affected by the sampling duration, but the particle diameters were different. We will clarify it by including the below sentences in the revised manuscript:

“EPFR concentrations contained in particles within the diameter of 50 nm – 3.2  $\mu\text{m}$  collected for 48 h during 26-27 June 2015 was  $\sim 2.2 \times 10^{11}$  spins  $\mu\text{g}^{-1}$ . EPFR concentrations contained in particles

within the diameter of 56 – 560 nm averaged over the entire measurement period was  $2.0(\pm 1.3) \times 10^{11}$  spins  $\mu\text{g}^{-1}$ .”

Page 6, Line 176: Is it 41

Response:

Carbon-centred radicals are reduced to 40% in the 1  $\mu\text{m}$  stage. Thanks for point out this typo, we will correct it in the revised manuscript.

Page 6, Line 201: What are the units here for ROS, is it spins/ $\mu\text{g}$ ?

Response:

The unit is  $\mu\text{g}^{-1}$  and not spins  $\mu\text{g}^{-1}$ , as  $\text{H}_2\text{O}_2$  is not radical, but it can be still directly compared with concentrations of EPFR and radical forms of ROS (in the unit of spins  $\mu\text{g}^{-1}$ ) as measured in this study.

Page 7, Line 203-215: I think the authors are completely confused here. DTT assay doesn't measure the ROS in the particle, rather the capability of particles to generate ROS in surrogate biological environment. I am not clear what the authors want to deduce in this discussion and what is the significance of this number of  $(2-7) \times 10^{14}$   $\mu\text{g}^{-1}$  of DTT molecules? It is important to note that DTT activity is a completely arbitrary unit and depends on the initial DTT concentration used in the assay.

Response:

The DTT assay measures the consumption rate of DTT molecules due to reactions of redox-active components of particulate matter with antioxidants. The total number of DTT molecules consumed per unit of mass and time are measure of the redox activity or oxidative potential of chemical compounds contained in the particles. The underlying assumption of the DTT assay is that the consumption of one DTT molecule would lead to the generation of one ROS molecule (e.g.,  $\text{H}_2\text{O}_2$ ). We agree that this assumption has not proved robustly and we are actually planning to investigate this aspect in details in the follow-up study. We think it is still meaningful to make this comparison, but we will refine the sentence to avoid confusion in the revised manuscript.

Page 8, Line 237: Can the authors add references showing HULIS is known to contain substantial amount of quinones?

Response:

We have added the following reference:

Verma, V., Wang, Y., El-Afifi, R., Fang, T., Rowland, J., Russell, A. G., and Weber, R. J.: Fractionating ambient humic-like substances (HULIS) for their reactive oxygen species activity – Assessing the importance of quinones and atmospheric aging, *Atmos. Environ.*, 120, 351-359, 2015.

Page 10, Line 308-310: I don't think that this study shows that ROS can be generated in lung fluid. I think again the authors are confusing between ROS activity (capability of particles to generate ROS) vs. ROS on the particles (measured in this study).

Response:

As pointed out, this study itself did not show that ROS can be generated in the lung lining fluid containing antioxidants, but it did show that the particles can form ROS in water. Several previous studies have shown that redox-active components such as transition metals and quinones can induce formation of ROS species upon interactions with lung antioxidants (Charrier et al., 2014; Charrier and Anastasio, 2011). We will clarify it in the revised manuscript as below:

“Previous studies have shown that redox-active components such as transition metals and quinones can induce ROS formation in surrogate lung lining fluid upon interactions with antioxidants (Charrier et al., 2014; Charrier and Anastasio, 2011). This study also implies that ROS may be released in lung lining fluid upon inhalation and respiratory deposition of atmospheric aerosol particles.”

#### **References:**

Charrier, J. G., and Anastasio, C.: Impacts of antioxidants on hydroxyl radical production from individual and mixed transition metals in a surrogate lung fluid, *Atmos. Environ.*, 45, 7555-7562, 2011.

Charrier, J. G., McFall, A. S., Richards-Henderson, N. K., and Anastasio, C.: Hydrogen Peroxide Formation in a Surrogate Lung Fluid by Transition Metals and Quinones Present in Particulate Matter, *Environ. Sci. Technol.*, 48, 7010-7017, 2014.

Birben, E., Sahiner, U. M., Sackesen, C., Erzurum, S., and Kalayci, O.: Oxidative stress and antioxidant defense, *World Allergy Organization Journal*, 5, 1, 2012.

Pryor, W. A., Squadrito, G. L., and Friedman, M.: The cascade mechanism to explain ozone toxicity - The role of lipid ozonation products, *Free Radical Biol. Med.*, 19, 935-941, 1995.

Winterbourn, C. C.: Reconciling the chemistry and biology of reactive oxygen species, *Nature Chem. Biol.*, 4, 278-286, 2008.

## Response to the comment to the Anonymous Referee #2

This study reports concentrations of particle-bound environmentally persistent free radicals (EPFR) and radical forms of reactive oxygen species (ROS) using electron paramagnetic resonance (EPR) spectroscopy. ROS species quantified after release by extraction of submicron particle samples in water include OH, O<sub>2</sub><sup>-</sup>, carbon- and oxygen-centered organic radicals; the authors further report concentrations as a function of particle size. The study proposes that the formation of ROS is due to the decomposition of organic hydroperoxides interacting with semiquinones in soot and/or HULIS particles, while EPFR are likely from semiquinone radicals. The study is well written and relevant to the atmosphere and human health concerns. I recommend publication in ACP after the following questions and comments are addressed.

Response:

We thank the referee for review and very positive evaluation of this manuscript.

Comments:

-How do the concentrations of ROS (spins  $\mu\text{g}^{-1}$ ) compare to those previously reported? It may be useful to include a note in the Methods section about the context of these units in terms of their relationship to standard particle concentrations.

Response:

This study provided the concentrations of radical forms of ROS (e.g., sum of OH, O<sub>2</sub><sup>-</sup>, C- and O-centered organic radicals), which is the first measurement to the best of our knowledge. Thus, we cannot make direct comparison with previous studies. Instead, we have made comparison with previous measurements of redox activity and oxidative potential of PM by the dichlorofluorescein (DCFH) and dithiothreitol (DTT) assays, as discussed in Sect. 3.2. Assuming that the consumption of one DTT molecule would correspond to the generation of one ROS molecule (e.g., H<sub>2</sub>O<sub>2</sub>), these values are about a few orders of magnitude higher than concentrations of radical forms of ROS measured in this study. This is reasonable as H<sub>2</sub>O<sub>2</sub> is closed shell and much more stable than open-shell radical ROS. The standard unit for the particle mass concentration is  $\mu\text{g m}^{-3}$ , which indicates  $\mu\text{g}$  of particle mass in 1 m<sup>3</sup> of air; whereas the unit (spins  $\mu\text{g}^{-1}$ ) of ROS or EPFR concentrations used in this study indicates the number of spins (or radicals) per unit of particle mass. We will clarify this point in the method section of the revised manuscript.

-A mention of g-factor before the Results section may be helpful as written it is difficult to understand the importance of the parameter and how unique a g-factor is to each measurable species.

Response:

Thanks for your suggestion. We will add the following sentence in the method section:

“Paramagnetic species are characterized based on their g-factor values. Free electrons have a g-factor value of 2.0023 and organic radicals have higher g-factor values (2.0030 – 2.0060), depending on the number of oxygen atom in the molecule (B. Dellinger et al. 2007)”

-Figure 1 - what does the structure at 560 nm indicate?

Response:

The spectrum for 560 nm particles indicates that no radicals have been found for this size range particles. The high background, probably due to metal oxides, causes the spectrum to be steep in shape and the fine structure seems to be not significant.

-Lines 83-98. Can you expand a bit on any transmission effects of the impactor, especially for the coarse particles?

Response:

For impactor such as MOUDI, the transmission effect of particles collected on a stage is considered to be a step function with boundaries of the steps corresponding to the cut-off sizes of the upper and lower stages. That is, each stage has an efficiency of 50% in collecting particles with the diameter comparable to its nominal cut-off size. The collection efficiency reaches 100% for particles with diameter just bigger than the nominal cut-off size of the upper stage (Marple et. al. 1991). However, the collection efficiency of particles with the diameter comparable to the nominal cut-off size of a stage can be lower than 50% due to bouncing effects. Due to bouncing, particles that are supposed to impact on a stage can be transferred to the next stage. This process is much more influential for particles in the coarse fraction. We will add the below sentence in the revised manuscript:

“Note that transmission and bouncing effects may cause mixing of particles exhibiting relatively different sizes on one stage, particularly for coarse particles (Gomes et al., 1990; Bateman et al., 2014).”

-Figure 2. What do the error bars indicate? Is there any significance that both ROS and EPFR have minima at the same size (560 nm)?

Response:

The error bars represent standard errors based on uncertainties of the particle mass and signal integration of EPR spectra. We will add this information in the figure caption. The minimum in the EPFR and ROS concentration for particles at 560 nm is likely due to a low mass loading in this stage.

-Lines 99-113. What are the background concentrations of these species? Is there any signal when EPFR are not present?

Response:

Blank measurements confirmed that there are no background concentrations of EPFR. In the absence of EPFR, the signal is just a horizontal line, when the concentrations of other paramagnetic species (e.g., transition metals) are below the detection limit.

-Figure 3. Can the authors expand on why rain events do not seem to dampen concentrations of EPFR in 100 nm particles as much as 180 nm particles?

Response:

EPFR concentrations in both 100 and 180 nm particle decreased substantially after rain events on May 30 (Saturday), but it was not very obvious, on June 1 (Monday), 2015. EPFR concentrations are controlled by both emission and deposition. The road traffic can be a main contributor of  $PM_{2.5}$  in the area around the sampling site and it is generally very limited during the weekend. This means that emission or production rates of EPFR on June 1 must be higher than on May 30. Moreover, scavenging efficiency of particles depends on rainfall intensity and sizes of rain droplet and particle (Seinfeld & Pandis, 2006), which might have caused the difference for 100 and 180 nm particles.

Figure 5. The authors may find it useful to note the total ROS concentrations to further illustrate the size dependence. For the largest particles (1.8  $\mu m$  especially), OH seemingly dominates the total ROS concentrations

Response:

The total ROS concentrations as a function of the particle diameter are shown as the red line in Figure 2. Figure 5 shows the relative contribution of each type of ROS to the total amount of ROS at each stage.

-did OH significantly contribute to the total ROS concentration at 1.8  $\mu\text{m}$  or is this due to the smaller ROS concentrations skewing the total contributions of each species?

Response:

Yes, OH contributed up to about 90 % of the total ROS released by 1.8  $\mu\text{m}$  particles.

-Lines 308-319. Is our lung capacity inhalation dependent on the total concentration (spins  $\mu\text{g}^{-1}$ ) of these ROS/EPFR species? Is there an amount of ROS/EPFR that our lungs can safely inhale without potential health harm?

Response:

This is a very interesting and important question to be addressed. We have recently reported that fine particulate matter (PM<sub>2.5</sub>) containing redox-active transition metals, quinones, and secondary organic aerosols can increase ROS concentrations in the lung lining fluid to levels characteristic for respiratory diseases (~100 nM) (Lakey et al., 2016). Further studies are required to unravel threshold concentrations of ROS/EPFR that are harmful to human health. We will add this aspect in the revised manuscript.

References:

Dellinger B., Lomnicki S., Khachatryan L., Maskos Z., Hall R. W., Adoukpe J., McFerrin C., Truong H.: *Proceed. Combust. Inst.*, 31, 521, 2007

Bateman, A. P., Belassein, H., and Martin, S. T.: *Impactor Apparatus for the Study of Particle Rebound: Relative Humidity and Capillary Forces*, *Aerosol Sci. Technol.*, 48, 42-52, 2014.

Gomes, L., Bergametti, G., Dulac, F., and Ezat, U.: *Assessing the actual size distribution of atmospheric aerosols collected with a cascade impactor*, *J. Aerosol Sci.*, 21, 47-59, 1990.

Lakey, P. S. J., Berkemeier, T., Tong, H., Arangio, A. M., Lucas, K., Pöschl, U., and Shiraiwa, M.: *Chemical exposure-response relationship between air pollutants and reactive oxygen species in the human respiratory tract*, *Sci. Rep.*, 6, 32916, 2016.

Seinfeld, J. H., and Pandis, S. N.: Atmospheric chemistry and physics - From air pollution to climate change, John Wiley & Sons, Inc., New York, 2006.

Gehling W., Dellinger B.: Environmentally Persistent Free Radicals and Their Lifetime in PM2.5, Environ. Sci. Tech., 47(15), 8172, 2013

### Response to the comment to the Anonymous Referee #3

In this study, the authors report size-resolved measurements of EPFR and ROS radicals using EPR spectroscopy and LC-MS for samples collected for one week in Mainz as a demonstration. They show size-dependent variations in the proportion of radicals of ROS and EPFR, with concentrations of both peaking in the accumulation mode, and find that carbon-centered radicals contribute the largest proportions to radical species in ROS for PM1. Using laboratory generated spectra, they further propose that mechanisms for ROS generation in these samples require a combination of transition metals with organic hydroperoxides and quinones. The work is of high technical quality with important implications for understanding atmospheric processes and air quality, and the manuscript is well-written. The work is thus recommended for publication in Atmospheric Chemistry and Physics after the following comments have been addressed.

Response:

We thank the referee for review and very positive evaluation of this manuscript.

General comments regarding the measurement method:

1. Are there any transformation artifacts from the initial measurement of EPFR? For example, if the authors use collocated measurements and analyze ROS directly on the second filter, would they expect to find the same ROS concentrations measured after the filter has been used for quantification of EPFR?

Response:

EPR measurements for the EPFR detection are non-destructive measurements. The microwave radiation used during EPR analysis does not induce any changes in the chemical composition of the sample itself. Indeed, the intensity EPFR signal did not change when monitored over the experimental time. Thus, initial EPFR measurements would not affect subsequent ROS measurements of particle extracts in water.

2. On p.3, line 95, it is stated that "BMPO is an efficient spin-trapping agent [...]." Is the efficiency effectively considered to be 100% for all, or are there biases for certain radicals?

Response:

BMPO is known as a very efficient trapping agent for OH radicals (Tong et al., 2016). In this work, BMPO is assumed to have the same efficiency for all type of radicals. Even though there is no

thorough quantitative data specifically for BMPO trapping efficiency for superoxide and organic radicals, Sueishi et al. (2015) have reported that nitron-based spin traps have the highest reactivity towards OH and somewhat lower reactivity towards organic radicals and superoxide. Further studies are required to fully address this issue and we will note include the below sentence in the revised manuscript.

3. In the drying process with N<sub>2</sub>, is it possible that negative artifacts are introduced? How is the dried extract introduced into the EPR spectrometer?

Response:

The text was misleading. The water extracts were exposed to a N<sub>2</sub> flow to reduce the volume of the solution to 50 μL. 20 μL are then introduced into a glass capillary for EPR analysis. As N<sub>2</sub> is inert towards BMPO-trapped radicals, we do not think artifacts would be introduced. We will clarify it in the revised manuscript.

4. Is the detection limit reported the instrument detection limit, or analytical detection limit derived from blanks?

Response:

The reported detection limit refers to the detection limit of the instrument.

General comments regarding the reported concentrations:

1. Would it be meaningful to plot radiation intensity alongside Fig. 3 to discuss the potential role of photochemistry? For instance, on 02/06/2015, the concentration is also high even though the conditions are presumably cloudy according to descriptions in text. In this regard, the radical concentrations appear to depend on many factors and underscores the benefit of integrating this technique into larger measurement campaigns.

Response:

This is a very good idea as photochemistry may be related to EPFR formation; however, unfortunately we do not have data of radiation intensity.

2. Are the proportions in Fig. 5 meant to be representative of those observed during the entire measurement campaign?

Response:

The proportions in Fig. 5 are referred to samples collected for 48h in June 2015 and extracted in presence of BMPO. We will clarify it in the revised manuscript.

Minor comments:

1. p. 3, line 92: The authors discuss pre-cleaning and weighing, and then discuss particle extraction. It would be helpful if the description were explicit in the pre-sampling and post-sampling procedures.

Response:

Following your suggestion, we will describe explicitly the pre-sampling and the post-sampling procedures as follow:

“Particles were collected on 47 mm diameter Teflon filters (100 nm pore size, Merck Chemicals GmbH). Before sampling, each filter was cleaned and sonicated for 10 min with pure ethanol and ultra-pure water and dried with nitrogen gas before weighing. Teflon filters were weighed four times using a balance (Mettler Toledo XSE105DU) and mounted in the MOUDI. After the sampling, each filter has been conditioned for at least one hour in the lab atmosphere (22 C and 40-50 RH) and weighted four times.”

2. p. 5, line 152: This is just a semantic issue, but it would seem more appropriate to say that the values in this work are comparable with the EPFR concentrations measured by Shaltout et al. (2015) - instead of the other way around - since their work preceded this one and sets the precedent to which following studies should be compared.

Response:

Following your comment, we will revise the sentence in the revised manuscript.

3. In the conclusions, the measurement location and period should be restated so the reported concentrations are placed in the proper context.

Response:

We thank referee 3 for pointing this out. We will include this information.

References.

Tong, H., Arangio, A. M., Lakey, P. S. J., Berkemeier, T., Liu, F., Kampf, C. J., Brune, W. H., Pöschl, U., and Shiraiwa, M.: Hydroxyl radicals from secondary organic aerosol decomposition in water, *Atmos. Chem. Phys.*, 16, 1761-1771, 2016.

## Response to the comment to the Anonymous Referee #4

This paper describes measurements of the concentrations of reactive species embedded in atmospheric aerosol collected from the roof of the MPI. It is a followup to the earlier paper this year by Tong et al which compared field samples to lab samples collected for a shorter period of time and focused on OH generation. The measurement method consists of extracting soluble molecules from the particles and reacting them with a scavenger. This is essentially a physical chemistry paper and my comments are from that perspective. This paper will be publishable after some edits to respond to the following comments.

Response:

We thank the referee for review and positive evaluation of this manuscript.

I found the terminology used by the authors to be confusing in places. Through use of words such as “we have also characterized and quantified ROS including OH, superoxide (O<sub>2</sub><sup>-</sup>) and carbon- and oxygen-centered organic radicals, which were released upon extraction of the particle samples in water.” the reader could conclude that the radicals are persistently present in the particle, rather than being formed by reaction of water with precursors during the extraction process and later scavenged. The multiple chemical steps involved in the experiment lend an ambiguity to how to relate the lab processes that are responsible for formation of detectable spins to atmospheric and physiological processes. As another example, on pages 4-5 the authors talk about spins per microgram but do not define this quantity. I presume they mean spins detected by extraction from a sample of this mass using the protocol described. The concentration of the scavenger is not given so it is not clear how closely this process is controlled or how repeatable it is. Clarification of the terminology and relation of the experimental conditions to those found in the lung and in clouds, for example, would be helpful.

Response:

Following your suggestion, we will make it clear that we measured ROS formed upon extraction into water throughout the revised manuscript. The unit for EPFR and ROS concentrations used in this study is spins  $\mu\text{g}^{-1}$ , which indicates the number of spins (or radicals) produced per unit of particle mass. We will add the following sentence in the revised manuscript.

“Concentrations of EPFR and ROS are reported in the unit of spins  $\mu\text{g}^{-1}$ , which indicates the number of spins (or radicals) per  $\mu\text{g}$  of particle mass.”

The concentration of the scavenger was specified in the method section (350  $\mu\text{L}$  of 20 mM BMPO was used). The experimental procedure was controlled well and repeatable (e.g., Tong et al., 2016).

(2) Only particles smaller than 1 micron contain extractable ROS material. Do the authors understand why this is? Since peroxides are photo labile I might have expected the opposite - the larger, more optically opaque particles would have more precursors than the smaller ones assuming the extraction processes work the same way for all particle sizes. Some discussion of the size effects would be useful.

Response:

ROS concentrations are indeed smaller for particles in the coarse mode, but ROS were formed also by particles larger than 1  $\mu\text{m}$ , as shown by the red line in Fig. 2, Fig. 4a and Fig. 5. The size-dependence was discussed in L266 – 273 (“SOA particles, which may contain large amounts of organic hydroperoxides, account for a major fraction in PM1 (Jimenez et al., 2009). SOA compounds may also coat coarse particles such as biological particles (Pöhlker et al., 2012). As shown in Fig. 2, semiquinones are mostly contained in submicron particles but not in coarse particles. Thus, the release of a variety of ROS species are most likely due to the interactions of organic hydroperoxides, semiquinones, and transition metal ions, whereas the dominance of OH radicals in coarse particles may be due to the decomposition of organic hydroperoxides in the absence of semiquinones.”).

(3) The reactive oxygen species released and scavenged during the analytical protocol are well known to have rich chemistry in water and very different reactivities compared to each other. Have the authors determined how efficiently are they being detected (absolute and relative values)?

Response:

We are aware that ROS chemistry is quite complex. We are currently making efforts on synthesizing possible reactions involving ROS, organic hydroperoxides, quinones and transition metals and developing the kinetic model. We intend to present these results in the follow-up study. Regarding the detection efficiency of ROS, BMPO is known as a very efficient trapping agent for OH radicals (Tong et al., 2016). In this work, BMPO is assumed to have the same efficiency for all type of radicals. Even though there is no thorough quantitative data specifically for BMPO trapping efficiency for superoxide and organic radicals, Sueishi et al. (2015) have reported that nitron-based spin-traps have the highest reactivity towards OH followed by carbon-centered radicals, oxygen-

centered organic radicals, and superoxide. Further studies are required to fully address this issue and we will note include the below sentence in the revised manuscript.

(4) On page 9 line 269ff there is a section discussing implications for aerosol chemistry and lung chemistry. Since there are no data in this paper specifically looking at these implications but there are in Tong I recommend the reader referred back to the earlier paper instead.

Response:

Yes, we refer this aspect to Tong et al., (2016). This study itself did not show that ROS can be generated in the lung lining fluid containing antioxidants, but it did show that the particles can form ROS in water. Several previous studies have shown that redox-active components such as transition metals and quinones can induce formation of ROS species upon interactions with lung antioxidants (Charrier et al., 2014; Charrier and Anastasio, 2011). We will clarify it in the revised manuscript as below:

“Previous studies have shown that redox-active components such as transition metals and quinones can induce ROS formation in surrogate lung lining fluid upon interactions with antioxidants (Charrier et al., 2014; Charrier and Anastasio, 2011). This study also implies that ROS may be released in lung lining fluid upon inhalation and respiratory deposition of atmospheric aerosol particles.”

#### **References.**

Tong, H., Arangio, A. M., Lakey, P. S. J., Berkemeier, T., Liu, F., Kampf, C. J., Brune, W. H., Pöschl, U., and Shiraiwa, M.: Hydroxyl radicals from secondary organic aerosol decomposition in water, *Atmos. Chem. Phys.*, 16, 1761-1771, 2016.

# 1 Quantification of environmentally persistent free radicals and reactive 2 oxygen species in atmospheric aerosol particles

3  
4 Andrea M. Arangio<sup>1</sup>, Haijie Tong<sup>1</sup>, Joanna Socorro<sup>1</sup>, Ulrich Pöschl<sup>1</sup> & Manabu Shiraiwa<sup>1,2\*</sup>

5 <sup>1</sup> Multiphase Chemistry Department, Max Planck Institute for Chemistry, Mainz, Germany

6 <sup>2</sup> Department of Chemistry, University of California, Irvine, CA, USA

7 \* [m.shiraiwa@uci.de](mailto:m.shiraiwa@uci.de)

## 8 9 10 11 **Abstract**

12 Fine particulate matter plays a central role in adverse health effects of air pollution.  
13 Inhalation and deposition of aerosol particles in the respiratory tract can lead to the release of  
14 reactive oxygen species (ROS), which may cause oxidative stress. In this study, we have  
15 detected and quantified a wide range of particle-associated radicals using electron  
16 paramagnetic resonance (EPR) spectroscopy. Ambient particle samples were collected using  
17 a cascade impactor at a semi-urban site in central Europe, Mainz, Germany in May – June  
18 2015. Concentrations of environmentally persistent free radicals (EPFR), most likely  
19 semiquinone radicals, were found to be in the range of  $(1 - 7) \times 10^{11}$  spins  $\mu\text{g}^{-1}$  for particles in  
20 the accumulation mode, whereas coarse particles with a diameter larger than 1  $\mu\text{m}$  did not  
21 contain substantial amounts of EPFR. Using a spin trapping technique followed by  
22 deconvolution of EPR spectra, we have also characterized and quantified ROS including OH,  
23 superoxide ( $\text{O}_2^-$ ) and carbon- and oxygen-centred organic radicals, which were **formed** upon  
24 extraction of the particle samples in water. Total ROS amounts of  $(0.1 - 3) \times 10^{11}$  spins  $\mu\text{g}^{-1}$   
25 were released by submicron particle samples and the relative contributions of OH,  $\text{O}_2^-$ , C-  
26 centred and O-centred organic radicals were ~11 - 31%, ~2 - 8%, ~41 - 72% and ~0- 25%,  
27 respectively, depending on particle sizes. OH was the dominant species for coarse particles.  
28 Based on comparisons of the EPR spectra of ambient particulate matter with those of  
29 mixtures of organic hydroperoxides, quinones and iron ions followed by chemical analysis  
30 using liquid chromatography mass spectrometry (LC-MS), we suggest that the particle-  
31 associated ROS were formed by decomposition of organic hydroperoxides interacting with  
32 transition metal ions and quinones contained in atmospheric humic-like substances (HULIS).

33

## 34 1. Introduction

35 Epidemiological studies have clearly shown positive correlations between respiratory  
36 diseases and ambient fine particulate matter (Pope and Dockery, 2006; Strak et al., 2012;  
37 West et al., 2016). A recent study has estimated that outdoor air pollution leads to 3.3 million  
38 premature deaths per year worldwide, which is mostly due to particular matter with a particle  
39 diameter less than 2.5  $\mu\text{m}$  ( $\text{PM}_{2.5}$ ) (Lelieveld et al., 2015). Plausible reasons include the  
40 cytotoxicity of ambient  $\text{PM}_{2.5}$  and its ability to induce inflammatory responses by oxidative  
41 stress causing functional alterations of pulmonary epithelial cells (Nel, 2005; Gualtieri et al.,  
42 2009). Oxidative stress is mediated by reactive oxygen species (ROS) including OH,  $\text{H}_2\text{O}_2$ ,  
43 superoxide ( $\text{O}_2^-$ ), as well as organic radicals (Pryor et al., 1995; Winterbourn, 2008; Birben et  
44 al., 2012; Pöschl and Shiraiwa, 2015). Upon PM deposition into the respiratory tract and  
45 interactions with lung antioxidants,  $\text{H}_2\text{O}_2$  can be generated by redox-active components  
46 contained in  $\text{PM}_{2.5}$  such as transition metals (Charrier et al., 2014; Fang et al., 2015),  
47 semiquinones (Kumagai et al., 1997; Cho et al., 2005; Khachatryan et al., 2011; McWhinney  
48 et al., 2013), and humic-like substances (Kumagai et al., 1997; Cho et al., 2005; Lin and Yu,  
49 2011; Charrier et al., 2014; Dou et al., 2015; Fang et al., 2015; Verma et al., 2015a).  $\text{H}_2\text{O}_2$   
50 can be converted into highly-reactive OH radicals via Fenton-like reactions with iron and  
51 copper ions (Charrier et al., 2014; Enami et al., 2014).

52 Ambient particles have been found to contain large amounts of ROS (mostly  $\text{H}_2\text{O}_2$ ) in  
53 the particle phase (Hung and Wang, 2001; Venkatachari et al., 2005; Venkatachari et al.,  
54 2007; Fuller et al., 2014). Substantial amounts of particle-bound ROS are found on biogenic  
55 secondary organic aerosols (SOA) produced from the oxidation of  $\alpha$ -pinene, linalool, and  
56 limonene (Chen and Hopke, 2010; Chen et al., 2011; Pavlovic and Hopke, 2011; Wang et al.,  
57 2011; Wang et al., 2012). Recently, Tong et al. (2016) have shown that terpene and isoprene  
58 SOA can form OH radicals upon interactions with liquid water and iron ions under dark  
59 conditions. This can be explained by the decomposition of organic hydroperoxides, which  
60 account for the predominant fraction of SOA mass and are generated via multigenerational  
61 oxidation and autoxidation (Docherty et al., 2005; Ziemann and Atkinson, 2012; Crouse et  
62 al., 2013; Ehn et al., 2014; Epstein et al., 2014; Badali et al., 2015).

63 In addition,  $\text{PM}_{2.5}$  contain environmentally persistent free radicals (EPFR) that can be  
64 detected directly by electron paramagnetic resonance (EPR) spectroscopy (Dellinger et al.,  
65 2001; Khachatryan et al., 2011; Gehling and Dellinger, 2013). EPFR are stable radicals with  
66 an e-folding lifetime exceeding one day (Gehling and Dellinger, 2013; Jia et al., 2016). The  
67 chemical nature of EPFR is remarkably similar to semiquinone radicals, which can be

68 stabilized via electron transfer with transition metals in the particle phase (Truong et al., 2010;  
69 Vejerano et al., 2011; Gehling and Dellinger, 2013). EPFR are formed upon combustion and  
70 pyrolysis of organic matter (Dellinger et al., 2001; Dellinger et al., 2007). The formation of  
71 stable radicals can also be induced by heterogeneous and multiphase chemistry of organic  
72 aerosols. Heterogeneous ozonolysis of aerosol particles such as polycyclic aromatic  
73 hydrocarbons (PAH) and pollen proteins can lead to the formation of long-lived reactive  
74 oxygen intermediates (ROI) (Shiraiwa et al., 2011; Shiraiwa et al., 2012; Reinmuth-Selzle et  
75 al., 2014; Borrowman et al., 2015; Kampf et al., 2015; Berkemeier et al., 2016).

76 In this work, ambient particles with a diameter in the range of 56 nm to 3.2  $\mu\text{m}$  were  
77 collected using a cascade impactor during May – July 2015 in Mainz, Germany. Size  
78 dependences of EPFR concentrations contained in ambient particles have been measured  
79 using an EPR spectrometer. Particles were also extracted in water containing a spin-trapping  
80 agent followed by EPR analysis to quantify the formation of various radical forms of ROS  
81 including OH, superoxide ( $\text{O}_2^-$ ) and carbon- and oxygen-centred organic radicals.

82

## 83 2. Methods

84 Ambient particles were collected using a micro-orifice uniform deposition impactor  
85 (MOUDI, 110-R mode, MSP Corporation) on the roof of the Max Planck Institute for  
86 Chemistry, Mainz, Germany (49.99 N, 8.23 E). The sampling was conducted every 24 h  
87 starting at 5 PM during 28 May - 9 June 2015. Particles were collected with a sampling time  
88 of 48 h during 26-27 June and 18-19 July 2015 **in order to collect sufficiently high mass**  
89 **loadings for all stages of different particle size ranges.** The sampling was conducted with a  
90 flow rate of 30 L  $\text{min}^{-1}$  with the following nominal lower cut-off particle diameters: 56, 100,  
91 180, 320, 560 nm, 1  $\mu\text{m}$ , and 1.8  $\mu\text{m}$ . **Note that transmission and bouncing effects might have**  
92 **caused mixing of particles exhibiting relatively different sizes on one stage, particularly for**  
93 **coarse particles (Gomes et al., 1990; Bateman et al., 2014).** Particles were collected on 47  
94 mm diameter Teflon filters (100 nm pore size, Merck Chemicals GmbH). **Before sampling,**  
95 **each filter was cleaned and sonicated for 10 min with pure ethanol and ultra-pure water and**  
96 **dried with nitrogen gas before weighing. Teflon filters were weighed four times using a**  
97 **balance (Mettler Toledo XSE105DU) and mounted in the MOUDI. After sampling, each**  
98 **filter has been conditioned for at least one hour (22-23  $^{\circ}\text{C}$  and 40-50 RH) and weighted four**  
99 **times before being folded and inserted in a 4 mm EPR tube.** Particles were extracted by  
100 immersing the filter into a solution containing 350  $\mu\text{L}$  of 20 mM 5-tert-Butoxycarbonyl-5-  
101 methyl-1-pyrroline-N-oxide (BMPO, high purity, Enzo Life Sciences GmbH) and stirred with

102 a vortex shaker (Heidolph Reax 1) for 7-9 min. BMPO is an efficient spin-trapping agent for  
103 OH, O<sub>2</sub><sup>-</sup> and organic radicals (Zhao et al., 2001; Tong et al., 2016). Note that the trapping  
104 efficiency of O<sub>2</sub><sup>-</sup> and organic radicals might be lower compared to OH radicals, as the recent  
105 study has reported that nitron-based spin traps have the highest reactivity towards OH and  
106 somewhat lower reactivity towards organic radicals and superoxide (Sueishi et al., 2015).  
107 Extracts were dried for approximately 14-17 min under 1-3 bar flow to reduce the volume of  
108 the solution to 50 μL and then 20 μL were used for EPR measurements.

109 A continuous-wave electron paramagnetic resonance (CW-EPR) X-band spectrometer  
110 (EMXplus-10/12, Bruker, Germany) was used for detection and quantification of stable  
111 radicals and ROS. Filters containing particles were folded and introduced into a 4 mm i.d.  
112 quartz tube and inserted directly into a high sensitivity cavity. EPR spectra were recorded at a  
113 room temperature of 23 °C by setting the following operating parameters: a modulation  
114 frequency of 100 kHz; a microwave frequency of 9.84 GHz; a microwave power of 2.149  
115 mW (20 db); a modulation amplitude of 1.0 G; a sweep width of 110.0 G; a sweep time of  
116 175 s; a receiver gain of 40 db; a time constant of 40.96 ms; a conversion time of 160 ms; and  
117 a scan number of 6. Paramagnetic species are characterized based on their g-factor values.  
118 Free electrons have a g-factor value of 2.0023 and organic radicals have higher g-factor  
119 values (2.0030 – 2.0060), depending on the number of oxygen atom in the molecule  
120 (Dellinger et al., 2007).

121 The spin-counting method embedded in the Bruker software Xenon was used to  
122 quantify detected radicals. The spin-counting method was calibrated using a standard  
123 compound 4-hydroxy-2,2,6,6-tetramethylpiperidin-1-oxyl (TEMPOL). The detection limit of  
124 EPR was  $\sim 1 \times 10^{10}$  spins μg<sup>-1</sup>. Concentrations of EPFR and ROS are reported in the unit of  
125 spins μg<sup>-1</sup>, which indicates the number of spins (or radicals) per μg of particle mass. For  
126 better quantification and determination of the relative contributions of OH, O<sub>2</sub><sup>-</sup>, carbon-  
127 centred and oxygen-centred organic radicals, EPR spectra were fitted and simulated using  
128 Xenon and the Matlab-based computational package Easyspin (Stoll and Schweiger, 2006).

129

### 130 **3. Results and discussion**

#### 131 **3.1. Environmentally persistent free radicals**

132 Figure 1 shows EPR spectra of ambient particles in the lower cut-off diameter range of  
133 56 nm – 1.8 μm. Fine particles, with lower cut-off diameters of 56 - 320 nm, show a single  
134 and unstructured peak with a g-factor of  $\sim 2.003$  and with a peak to peak distance ( $\Delta H_{p-p}$ )  
135 ranging from 3 to 8 G. Such spectra are characteristic for EPFR, which have been attributed

136 to semiquinone radicals (Dellinger et al., 2001; Dellinger et al., 2007; Vejerano et al., 2011;  
137 Bahrle et al., 2015). Particles with a diameter smaller than 56 nm and larger than 560 nm did  
138 not show significant signals, indicating the reduced amount of EPFR in these size ranges.  
139 EPR spectra for particles with the lower cut-off diameters of 56 – 320 nm for each sampling  
140 day are presented in Fig. A1.

141 The black line in Fig. 2 shows the size distribution of EPFR concentrations. Particles  
142 with different sizes had different radical contents and particles with the lower cut-off  
143 diameter of 100 nm contained the highest EPFR concentrations of  $7.0(\pm 0.7) \times 10^{11}$  spins  $\mu\text{g}^{-1}$ .  
144 High abundances of EPFR in particles in the accumulation mode is consistent with mass size  
145 distributions of combustion-generated particles such as soot or black carbon, which typically  
146 have peak concentrations around 100 – 200 nm (Bond et al., 2013). **This observation is in line  
147 with that EPFR may be often associated with soot particles (Dellinger et al., 2007).**

148 Figure 3 shows the temporal evolution of EPFR concentrations contained in particles  
149 with lower cut-off diameters of 100 and 180 nm. During the sampling period of two weeks,  
150 there were two rain events (on 30 May 2015 and 1 June 2015) and three sunny days (4-6 June  
151 2015), and the other days were cloudy. The mass concentrations of particles within the  
152 diameters of 56 - 560 nm were in the range of  $3.9 - 12.8 \mu\text{g m}^{-3}$ . Maximum values of  $\sim 7 \times$   
153  $10^{11}$  spins  $\mu\text{g}^{-1}$  were reached during sunny days, indicating that photochemistry may be  
154 related to EPFR production. For example, heterogeneous reactions of photo-oxidants  
155 including  $\text{O}_3$  and OH with soot or PAH may contribute to the formation of long-lived radicals  
156 (Shiraiwa et al., 2011; Borrowman et al., 2015). Radical concentrations were as low as  $6.3 \times$   
157  $10^{10}$  spins  $\mu\text{g}^{-1}$  during rain events, most likely due to low production of EPFR and scavenging  
158 by precipitation.

159 EPFR concentrations contained in particles **within the diameter of 50 nm – 3.2  $\mu\text{m}$**   
160 collected for 48 h during 26-27 June 2015 was  $\sim 2.2 \times 10^{11}$  spins  $\mu\text{g}^{-1}$ . EPFR concentrations  
161 contained in particles within the diameter of 56 – 560 nm averaged over the entire  
162 measurement period was  $2.0(\pm 1.3) \times 10^{11}$  spins  $\mu\text{g}^{-1}$ . Squadrito et al. (2001) determined the  
163 EPFR concentrations to be in the range of  $(1-10) \times 10^{11}$  spins  $\mu\text{g}^{-1}$  in  $\text{PM}_{2.5}$  sampled for 24 h  
164 in five different urban sites in the United States. Gehling et al. (2014) reported that the EPFR  
165 concentration was in the range of  $(7-55) \times 10^{10}$  spins  $\mu\text{g}^{-1}$  at a site in Louisiana near heavy  
166 interstate traffic along a major industrial corridor of the Mississippi River. Shaltout et al.  
167 (2015) measured radical concentrations in the range of  $(2-6) \times 10^{10}$  spins  $\mu\text{g}^{-1}$  in  $\text{PM}_{2.5}$   
168 collected in industrial-, residential- and traffic-dominated sites in Taif city, Saudi Arabia. **The**

169 EPFR concentrations measured in this work are comparable with these previous  
170 measurements.

171

### 172 3.2. Reactive oxygen species

173 Figure 4a shows EPR spectra of ambient particles with lower cut-off diameters of 56  
174 nm - 1.8  $\mu\text{m}$  extracted in water with the spin-trapping agent BMPO. Each EPR spectrum is  
175 composed of several overlapped lines, originating from different radical forms of ROS.  
176 Dashed lines indicate the positions of each peak for each type of trapped ROS including OH  
177 (green), superoxide (red), carbon-centred (orange) and oxygen-centred organic radicals (blue).  
178 The relative abundance of these radicals was different for each size range, causing the EPR  
179 spectral features to be highly variable. For example, spectra from particles larger than 1.0  $\mu\text{m}$   
180 consist mainly of four peaks that are typical for OH radicals, whereas those for smaller  
181 particles contain more peaks indicating the presence of multiple radicals.

182 To estimate the relative amount of each type of ROS, the observed EPR spectra were  
183 fitted and simulated using the software Easyspin 5.0 and Xenon. Four types of radicals have  
184 been used to fit the spectra: BMPO-OH (hyperfine coupling constants of  $a^{\text{N}} = 14.3 \text{ G}$ ,  $a^{\text{H}}_{\beta} =$   
185  $12.7 \text{ G}$ ,  $a^{\text{H}}_{\gamma} = 0.61 \text{ G}$ ), BMPO-OOH ( $a^{\text{N}} = 14.3 \text{ G}$ ,  $a^{\text{H}} = 8.1 \text{ G}$ ), BMPO-R ( $a^{\text{N}} = 15.2 \text{ G}$ ,  $a^{\text{H}} =$   
186  $21.6 \text{ G}$ ) and BMPO-OR ( $a^{\text{N}} = 14.5 \text{ G}$ ,  $a^{\text{H}}_{\beta} = 16.6 \text{ G}$ ). As shown in Fig. 4b, the simulated EPR  
187 spectrum reproduced the observed spectrum very well with a small residual. The  
188 deconvolution of spectra allowed us to estimate the relative contribution of four types of ROS  
189 within each particle size range.

190 Figure 5 shows the relative contributions of OH (green), superoxide (red), carbon-  
191 centred (orange) and oxygen-centred (blue) organic radicals to the total radicals trapped by  
192 BMPO in [water extracts of particles collected for 48 h during 26-27 June 2015](#). Carbon-  
193 centred radicals are the most abundant type of radicals, contributing ~50 - 72% of total ROS  
194 for PM1. It decreases to 41% and 9% for particles with lower cut-off diameters of 1  $\mu\text{m}$  and  
195 1.8  $\mu\text{m}$ , respectively. The OH radical accounts for ~11 - 31% of total trapped radicals for  
196 PM1, whereas OH was the dominant species for coarse particles with diameters of 1.8 - 3.2  
197  $\mu\text{m}$ . The least abundant radical for all size ranges was  $\text{O}_2^-$ , with contributions of ~2 - 8% and  
198 without any clear size dependence. The amount of oxygen-centred organic radicals ranges  
199 between 12% and 25% in particles with a diameter below 1  $\mu\text{m}$  and its contribution was  
200 negligible for coarse particles. Note that the contribution of oxygen-centred organic radicals  
201 for particles with a diameter of 1 - 1.8  $\mu\text{m}$  might be attributed to the OH radical: the  
202 hyperfine coupling constants for BMPO-OR for better fitting the spectrum for this size range

203 needed to be changed slightly ( $a^N = 13.5$  G,  $a^H_\beta = 15.3$  G,  $a^H_\gamma = 0.6$  G). These values are  
204 similar to constants of a second conformer of BMPO-OH.

205 The red line in Fig. 2 shows the size-dependent concentrations of radical forms of ROS  
206 (e.g., sum of OH,  $O_2^-$ , C- and O- centred organic radicals). Particles with the lower cut-off  
207 diameter of 100 nm have the highest ROS concentrations of  $2.7(\pm 0.2) \times 10^{11}$  spins  $\mu\text{g}^{-1}$ .  
208 Concentrations are smaller for particles in the coarse mode with a diameter larger than 1  $\mu\text{m}$ .  
209 This is consistent with previous studies, suggesting that particles in the accumulation mode  
210 are the most active in ROS generation (Hung and Wang, 2001; Venkatachari et al., 2007;  
211 Saffari et al., 2013; Wang et al., 2013; Saffari et al., 2014). The total concentration of radical  
212 forms of ROS was measured to be  $1.2 \times 10^{11}$  spins  $\mu\text{g}^{-1}$ . Note that  $O_2^-$  concentrations might  
213 be underestimated as the lifetime of the BMPO-OOH adduct is relatively short (~20 min)  
214 (Ouari et al., 2011; Abbas et al., 2014).

215 Previous studies have measured redox activity and oxidative potential of PM by the  
216 dichlorofluorescein (DCFH) and dithiothreitol (DTT) assays. The DCFH assay is mostly  
217 sensitive to  $H_2O_2$  and other peroxides. For example, Hung and Wang (2001) reported ROS  
218 concentrations as  $1 \times 10^{13}$   $\mu\text{g}^{-1}$  in Taipei, Taiwan. This value is very similar to  $H_2O_2$   
219 concentrations contained in ambient  $PM_{2.5}$ , which has been quantified to be up to  $1 \times 10^{13}$   $\mu\text{g}^{-1}$   
220 in an urban environment in southern California using HPLC fluorescence (Wang et al., 2012).  
221 The DTT assay is based on the decay of DTT due to redox reactions with PM components,  
222 reporting the oxidative potential of PM in moles of DTT consumed per unit of time and mass  
223 of PM. Verma et al. (2015b) and Fang et al. (2015) reported that  $PM_{2.5}$  sampled in an urban  
224 environment in Atlanta, Georgia, USA has a DTT activity in the range of 10-70  $\text{pmol min}^{-1}$   
225  $\mu\text{g}^{-1}$ . Assuming an integration time of 20 min needed for the extraction of PM in this work,  
226 this value corresponds to  $(1-8) \times 10^{14}$   $\mu\text{g}^{-1}$  of DTT molecules consumed. Charrier et al. (2012)  
227 also reported that  $PM_{2.5}$  sampled in an urban environment in Fresno, California USA has a  
228 DTT activity of 27 - 61  $\text{pmol min}^{-1} \mu\text{g}^{-1}$ , corresponding to  $(2 - 7) \times 10^{14}$   $\mu\text{g}^{-1}$  of DTT molecules  
229 consumed in 20 min. Assuming that the consumption of one DTT molecule would  
230 correspond to the generation of one ROS molecule (e.g.,  $H_2O_2$ ), these values are about a few  
231 orders of magnitude higher than concentrations of radical forms of ROS measured in this  
232 study. This is reasonable as  $H_2O_2$  is closed shell and much more stable than open-shell radical  
233 forms of ROS.

234

### 235 3.3. ROS formation mechanism

236 It has been shown that semiquinones and reduced transition metals including Fe(II) and  
237 Cu(I) can react with O<sub>2</sub> to form O<sub>2</sub><sup>-</sup>, which can be further converted to H<sub>2</sub>O<sub>2</sub> (Gehling et al.,  
238 2014; Fang et al., 2015). Fenton-like reactions of H<sub>2</sub>O<sub>2</sub> with Fe(II) or Cu(I) can lead to the  
239 formation of OH radicals (Winterbourn, 2008; Pöschl and Shiraiwa, 2015). OH radicals can  
240 also be generated by the decomposition of organic hydroperoxides (ROOH) contained in  
241 SOA, yielding RO radicals (Tong et al., 2016). Several studies have reported a metal-  
242 independent decomposition of hydroperoxides and organic hydroperoxides driven by  
243 substituted quinones producing RO radicals (Sanchez-Cruz et al., 2014; Huang et al., 2015).  
244 The presence of Fe(II) or quinones is suggested to enhance ROOH decomposition and the  
245 formation of RO and OH radicals (Zhu et al., 2007a; Zhu et al., 2007b; Zhu et al., 2009;  
246 Sanchez-Cruz et al., 2014). Organic peroxides (ROOR) do not yield OH and RO radicals  
247 even in the presence of iron ions (Tong et al., 2016).

248 Based on these previous studies and considering that ambient particles may contain  
249 quinones, organic hydroperoxides, and transition metals, the observed ROS formation may be  
250 caused by interactions of these chemical components. To further investigate this aspect,  
251 mixtures of organic hydroperoxides, quinones, and Fe(II) were analysed by EPR and liquid  
252 chromatography mass spectrometry (LC-MS). Two standard organic hydroperoxides, cumene  
253 hydroperoxide and tert-butyl hydroperoxide, were used. For quinones, p-benzoquinone and  
254 humic-like substances are used, as HULIS are known to contain substantial amounts of  
255 quinones (Verma et al., 2015c).

256 Figure 6 shows the comparison of EPR spectra of ambient particles with a diameter of  
257 180 - 320 nm (black) sampled on 26 June 2015 (same as shown in Fig. 4) and the above  
258 mixtures of organic compounds. Panel (a) includes EPR spectra of mixtures of all three  
259 different components (ROOH, quinone, metal) and panel (b) presents mixtures of two  
260 different components. All three of the organic mixtures in panel (a) resemble the EPR  
261 spectrum of ambient particles by reproducing almost all of the peaks. Particularly, the EPR  
262 spectrum of the mixture containing cumene hydroperoxide, humic acid and Fe(II) closely  
263 overlaps with the ambient particle EPR spectrum. Similarity of spectra between p-  
264 benzoquinone and HULIS suggests that the chemical nature of quinones and HULIS is very  
265 similar. Note that peaks related to the BMPO-OOH adduct at 3497 G and at 3530 G are more  
266 prominent in standard organic mixtures compared to ambient particles. This may be due to  
267 the relatively short lifetime of BMPO-OOH of ~23 min (Zhao et al., 2001), which is  
268 comparable to the extraction and mixing time of BMPO with the atmospheric particles (21 –  
269 28 min), during which BMPO-OOH may have decayed. The trapped radicals have been

270 further characterized by LC-MS, confirming the presence of OH and semiquinone radicals as  
271 well as carbon- and oxygen centred organic radicals, as detailed in Appendix A and Figs. A1  
272 and A2.

273 EPR spectra of mixtures containing two compounds in panel (b) reproduce only a part  
274 of the observed peaks. These observations strongly suggest that the combination of these  
275 three chemical components play an important role in generating ROS species by atmospheric  
276 particles. The role of transition metals is crucial to enhance radical formation, most likely via  
277 Fenton-like reactions (Tong et al., 2016) and by participating in redox-cycling of quinones  
278 (Khachatryan and Dellinger, 2011), as intensities of EPR spectra without Fe(II) (CHP +  
279 HULIS, dark blue; CHP + pBq, orange) are small. Carbon-centred radicals may have  
280 multiple sources such as the decomposition of the BMPO-OR adduct by scission of the  
281 carbon in  $\beta$  position, yielding for example  $\text{CH}_3$  radicals (Zhu et al., 2007b; Huang et al., 2015)  
282 as detected by LC-MS (Fig. A2). They may also be generated by secondary reactions of non-  
283 trapped OH radicals with water-soluble organic compounds.

284 SOA particles, which may contain large amounts of organic hydroperoxides, account  
285 for a major fraction in PM1 (Jimenez et al., 2009). SOA compounds may also coat coarse  
286 particles such as biological particles (Pöhlker et al., 2012). As shown in Fig. 2, semiquinones  
287 are mostly contained in submicron particles but not in coarse particles. Thus, the release of a  
288 variety of ROS species are most likely due to the interactions of organic hydroperoxides,  
289 semiquinones, and transition metal ions, whereas the dominance of OH radicals in coarse  
290 particles may be due to the decomposition of organic hydroperoxides in the absence of  
291 semiquinones.

292

#### 293 **4. Conclusions and implications**

294 In this study particle-associated environmentally persistent free radicals (EPFR) and  
295 radical forms of ROS have been quantified using electron paramagnetic resonance (EPR)  
296 spectroscopy. [Average EPFR concentrations were measured to be  \$\sim 2 \times 10^{11}\$  spins  \$\mu\text{g}^{-1}\$  in  
297 ambient particles collected in Mainz, Germany in May – June 2015.](#) The chemical identity of  
298 EPFR is likely to be semiquinone radicals based on the g-factors observed by EPR  
299 spectroscopy. We found that particles with different sizes had different radical contents and  
300 particles with a diameter of 100 - 180 nm had the highest abundance of EPFR, whereas  
301 coarse particles did not contain EPFR. This is consistent with the size distribution of  
302 combustion particles such as soot and humic-like substances (HULIS), which may contain  
303 substantial amounts of EPFR.

304 Reactive oxygen species (ROS) are **formed** upon extraction of particles into water.  
305 Particles with the diameter of 100 – 180 nm have released the highest ROS concentrations of  
306  $2.7(\pm 0.2) \times 10^{11}$  spins  $\mu\text{g}^{-1}$ . By deconvoluting the obtained EPR spectra, four types of radicals,  
307 including OH,  $\text{O}_2^-$ , carbon-centred and oxygen-centred organic radicals were quantified. The  
308 relative amounts of OH,  $\text{O}_2^-$ , C-centred and O-centred organic radicals in submicron particles  
309 were found to be ~11 - 31%, ~2 – 8%, ~41 – 72% and ~0- 25%, respectively, depending on  
310 the particle size. OH was the dominant species for coarse particles with a diameter larger than  
311 1  $\mu\text{m}$ . We suggest that the formation of these ROS species is due to the decomposition of  
312 organic hydroperoxides, which are a major component in SOA, interacting with  
313 semiquinones contained in soot or HULIS. ROS formation can be enhanced in the presence  
314 of iron ions by Fenton-like reactions.

315 These findings have significant implications for the chemical processing of organic  
316 aerosols in deliquesced particles and cloud water. The released OH radicals within particles  
317 or cloud droplets can oxidize other organic compounds, producing low-volatility products  
318 including organic acids, peroxides, and oligomers (Lim et al., 2010; McNeill et al., 2012;  
319 Ervens, 2015; Herrmann et al., 2015). Autoxidation in the condensed phase might be  
320 triggered by OH radicals forming highly oxidized compounds (Shiraiwa et al., 2014; Tong et  
321 al., 2016). High aqueous oxidant levels may cause fragmentation of organic compounds,  
322 resulting in an increased loss of carbon from the condensed phase (Daumit et al., 2016). The  
323 formed carbon- and oxygen-centred organic radicals are also expected to enhance chemical  
324 aging by participating in particle-phase chemistry involving aldehydes, carbonyls, and  
325 organic peroxides (Ziemann and Atkinson, 2012), although the exact role and impact of  
326 formed organic radicals are still unclear and subject to further studies.

327 Previous studies have shown that redox-active components such as transition metals  
328 and quinones can induce ROS formation in surrogate lung lining fluid upon interactions with  
329 antioxidants (Charrier and Anastasio, 2011; Charrier et al., 2014). This study also implies that  
330 ROS can be **formed** in lung lining fluid upon inhalation and respiratory deposition of  
331 atmospheric aerosol particles. Even though some fractions of ROS may be scavenged by  
332 antioxidants contained in lung lining fluid, excess concentrations of ROS including OH  
333 radicals, superoxide, and potentially also carbon- and oxygen centred organic radicals may  
334 cause oxidative stress to lung cells and tissues (Winterbourn, 2008; Pöschl and Shiraiwa,  
335 2015; Tong et al., 2016). Recently, Lakey et al. (2016) have shown that fine particulate  
336 matter containing redox-active transition metals, quinones, and secondary organic aerosols  
337 can increase ROS concentrations in the lung lining fluid to levels characteristic for

338 **respiratory diseases.** ROS play a central role in chemical transformation of biomolecules such  
339 as proteins and lipids in lung fluid to form damage associated molecular patterns (DAMPs),  
340 which can trigger immune reactions causing inflammation through the toll-like receptor  
341 radical cycle (Lucas and Maes, 2013). Due to the important implications to adverse aerosol  
342 health effects, further studies are warranted to characterize and quantify EPFR and ROS  
343 contained in atmospheric aerosol particles in various locations including highly polluted  
344 regions such as in East Asia and India.

345

#### 346 **Appendix A. LC-MS analysis of organic mixtures**

347 Two solutions of mixtures of standard organic hydroperoxides and quinones were  
348 analysed by liquid chromatography mass spectrometry (LC-MS). Solution (1) was the  
349 mixture of 200  $\mu\text{L}$  of p-benzoquinone solution at a concentration of  $0.2 \text{ g L}^{-1}$  (Reagent grade,  
350  $\geq 98\%$ , Sigma-Aldrich) in water (trace SELECT® Ultra, ACS reagent, for ultratrace analysis,  
351 Sigma-Aldrich), 100  $\mu\text{L}$  of Tert-Butyl hydroperoxide solution at a concentration of  $8.9 \text{ g L}^{-1}$   
352 (Luperox® TBH70X, 70 wt. %  $\text{H}_2\text{O}$ , Sigma-Aldrich) in water, 2.5  $\mu\text{L}$  of Iron (II) sulfate  
353 heptahydrate solution at  $0.3 \text{ g L}^{-1}$  (reagentPlus®,  $\geq 99\%$ , Sigma-Aldrich) in water and 1 mg of  
354 5-tert-Butoxycarbonyl-5-methyl-1-pyrroline-N-oxide (BMPO, high purity, Enzo Life  
355 Sciences GmbH). Solution (2) was the same as solution (1) but without Iron (II) sulfate  
356 heptahydrate. These solutions were stirred with a vortex shaker (Heidolph Reax 1) for 5  
357 minutes.

358 These solutions were analysed using a 1260 Infinity Bio-inert Quaternary LC system  
359 with a quaternary pump (G5611A), a HiP sampler (G5667A) and an electrospray ionization  
360 (ESI) source interfaced to a Q-TOF mass spectrometer (6540 UHD Accurate-Mass Q-TOF,  
361 Agilent). All modules were controlled by the MassHunter software (B.06.01, Agilent). The  
362 LC column was a Zorbax Extend-C18 Rapid resolution HT (2.1 x 50 mm, 1.8  $\mu\text{m}$ ) with a  
363 column temperature of 30 °C. The mobile phases were 3% (v/v) acetonitrile (HPLC Gradient  
364 Grade, Fisher Chemical) in water with formic acid (0.1 % v/v, LC-MS Chromasolv, Sigma-  
365 Aldrich) (Eluent A) and 3 % water in acetonitrile (Eluent B). The injection volume was 10  
366  $\mu\text{L}$ . The flow rate was  $0.2 \text{ mL min}^{-1}$  with a gradient program that starting with 3 % B for 3  
367 min followed by a 36 minutes step that raised eluent B to 60 %. Further, Eluent B was  
368 increased to 80 % at 40 minutes and returned to initial conditions within 0.1 minutes,  
369 followed by column re-equilibration for 9.9 min before the next run.

370 The ESI-Q-TOF instrument was operated in the positive ionization mode (ESI+) with a  
371 gas temperature of 325 °C, 20 psig nebulizer, 4000 V capillary voltage and 90 V fragmentor

372 voltage. During the full spectrum MS mode, no collision energy was used in order to collect  
373 species as their molecular ions. During MS/MS analysis employed for the structure  
374 determination, the fragmentation of protonated ions was conducted using the target MS/MS  
375 mode with 20 V collision energy. Spectra were recorded over the mass range of  $m/z$  50-1000.  
376 Data analysis was performed using qualitative data analysis software (B.06.00, Agilent).  
377 Blank solutions without BMPO were also prepared and analysed. Background signals were  
378 subtracted from the MS spectrum.

379 Figure A2 shows LC-MS/MS mass spectra of the products formed from the reaction of  
380 tert-butyl hydroperoxide, p-benzoquinone, BMPO in the presence of iron (solution 1). Very  
381 similar results were obtained for solutions in the absence of iron (solution 2). BMPO adducts  
382 with radicals  $\cdot\text{OH}$ ,  $\cdot\text{CH}_3$  and  $\cdot\text{OCH}_3$  were identified by LC-MS/MS. As shown in Figure  
383 A2(a.1), it was observed that ions at  $m/z$  160.0596, 216.1221 and 238.1020 were major ions  
384 formed in the positive mode. These protonated ions represent the  $[\text{BMPO}+\text{OH}-\text{C}_4\text{H}_8+\text{H}]^+$ ,  
385  $[\text{BMPO}+\text{OH}+\text{H}]^+$  and  $[\text{BMPO}+\text{OH}+\text{Na}+\text{H}]^+$  spin adducts, respectively. Figure A2 (a.2)  
386 displays the mass spectrum in the MS/MS mode for the fragmentation of the ion  $m/z$   
387 216.1221. Results confirmed the loss of the t-butoxycarbonyl function ( $-\text{C}_4\text{H}_8$ ), which is a  
388 characteristic fragment of BMPO, to form the ion  $m/z$  160.0585. The observed ion fragment  
389  $m/z$  114.0544, can be formed by the loss of  $\text{CH}_2\text{O}_2$ , as shown in Fig. A2(a.3). In Fig. A2(b.1),  
390 the spectrum showed the mass  $m/z$  158.0804 and 214.1431 that can be attributed to the  
391  $[\text{BMPO}+\text{CH}_3-\text{C}_4\text{H}_8+\text{H}]^+$  and  $[\text{BMPO}+\text{CH}_3+\text{H}]^+$ , respectively. The most abundant fragment  
392 ion ( $m/z$  158.0803) in the MS/MS mode confirmed the formation of BMPO+CH<sub>3</sub> adduct, as  
393 shown in Fig. A2(b.2). The peak  $m/z$  112.0752 can be formed by the loss of  $\text{CH}_2\text{O}_2$  (Fig.  
394 A2(b.3)). The spectrum in Fig. A2(c.1) shows major peaks at  $m/z$  174.0752, 230.1378 and  
395 252.1198, corresponding to  $[\text{BMPO}+\text{OCH}_3-\text{C}_4\text{H}_8+\text{H}]^+$ ,  $[\text{BMPO}+\text{OCH}_3+\text{H}]^+$  and  
396  $[\text{BMPO}+\text{OCH}_3+\text{Na}+\text{H}]^+$ , respectively. The formation of BMPO-OCH<sub>3</sub> was confirmed in  
397 MS/MS by the loss of the t-butoxycarbonyl functional group of BMPO to form the ion at  $m/z$   
398 174.0749 (panels (c.2) and (c.3)).

399 In addition, the radicals  $\text{C}_6\text{H}_5\text{O}_2\cdot$  or  $\cdot\text{C}_6\text{H}_5\text{O}_2$  and  $\text{C}_6\text{H}_9\text{O}_2\cdot$  or  $\cdot\text{C}_6\text{H}_9\text{O}_2$  were detected,  
400 although it was not possible to determine whether the chemical structure represented carbon-  
401 or oxygen-centred organic radicals using the applied method. Figure A3(a.1) shows the  
402 formation of protonated ions  $[\text{BMPO}+\text{C}_6\text{H}_5\text{O}_2+\text{H}]^+$  and  $[\text{BMPO}+\text{C}_6\text{H}_5\text{O}_2+\text{Na}+\text{H}]^+$  with  $m/z$   
403 308.1475 and 330.1298, respectively. The fragmentation in the MS/MS mode confirms the  
404 formation of BMPO+C<sub>6</sub>H<sub>5</sub>O<sub>2</sub> ( $m/z$  252.0855) that correspond to the loss of the characteristic  
405 t-butoxycarbonyl function as show in Fig. A3(a.2). The ion fragment observed  $m/z$  128.0702,

406 can be formed by the loss of C<sub>5</sub>O<sub>4</sub> (Figure A3(a.3)). Figure A3(b.1) shows the ion *m/z*  
407 312.1789, which can be attributed to the BMPO+C<sub>6</sub>H<sub>9</sub>O<sub>2</sub> spin adduct. Figure A3(b.2)  
408 suggests that the fragmentation of *m/z* 312.1789 to *m/z* 256.1166 by the loss of - C<sub>4</sub>H<sub>8</sub> (Figure  
409 A3(b.3)).

410

#### 411 **Acknowledgements.**

412 This study is funded by the Max Planck Society. We thank Christopher Kampf and Fobang  
413 Liu for helping LC-MS analysis and Pascale Lakey for helpful comments.

414

#### 415 **References.**

416 Abbas, K., Hardy, M., Poulhès, F., Karoui, H., Tordo, P., Ouari, O., and Peyrot, F.: Detection of  
417 superoxide production in stimulated and unstimulated living cells using new cyclic nitron spin traps,  
418 *Free Radical Biol. Med.*, 71, 281-290, 2014.

419 Badali, K. M., Zhou, S., Aljawhary, D., Antiñolo, M., Chen, W. J., Lok, A., Mungall, E., Wong, J. P.  
420 S., Zhao, R., and Abbatt, J. P. D.: Formation of hydroxyl radicals from photolysis of secondary  
421 organic aerosol material, *Atmos. Chem. Phys.*, 15, 7831-7840, 2015.

422 Bahrle, C., Nick, T. U., Bennati, M., Jeschke, G., and Vogel, F.: High-Field Electron Paramagnetic  
423 Resonance and Density Functional Theory Study of Stable Organic Radicals in Lignin: Influence of  
424 the Extraction Process, Botanical Origin, and Protonation Reactions on the Radical *g* Tensor, *The*  
425 *Journal of Physical Chemistry. A*, 119, 6475-6482, 2015.

426 Bateman, A. P., Belassein, H., and Martin, S. T.: Impactor Apparatus for the Study of Particle  
427 Rebound: Relative Humidity and Capillary Forces, *Aerosol Sci. Technol.*, 48, 42-52, 2014.

428 Berkemeier, T., Steimer, S., Krieger, U. K., Peter, T., Poschl, U., Ammann, M., and Shiraiwa, M.:  
429 Ozone uptake on glassy, semi-solid and liquid organic matter and the role of reactive oxygen  
430 intermediates in atmospheric aerosol chemistry, *Phys. Chem. Chem. Phys.*, 18, 12662-12674, 2016.

431 Birben, E., Sahiner, U. M., Sackesen, C., Erzurum, S., and Kalayci, O.: Oxidative Stress and  
432 Antioxidant Defense, *World Allergy Organization Journal*, 5, 1-11, 2012.

433 Bond, T. C., Doherty, S. J., Fahey, D. W., Forster, P. M., Bernsten, T., DeAngelo, B. J., Flanner, M.  
434 G., Ghan, S., Karcher, B., Koch, D., Kinne, S., Kondo, Y., Quinn, P. K., Sarofim, M. C., Schultz, M.  
435 G., Schulz, M., Venkataraman, C., Zhang, H., Zhang, S., Bellouin, N., Guttikunda, S. K., Hopke, P.  
436 K., Jacobson, M. Z., Kaiser, J. W., Klimont, Z., Lohmann, U., Schwarz, J. P., Shindell, D., Storelvmo,  
437 T., Warren, S. G., and Zender, C. S.: Bounding the role of black carbon in the climate system: A  
438 scientific assessment, *J. Geophys. Res.-Atmos.*, 118, 5380-5552, 2013.

439 Borrowman, C. K., Zhou, S., Burrow, T. E., and Abbatt, J. P.: Formation of environmentally  
440 persistent free radicals from the heterogeneous reaction of ozone and polycyclic aromatic compounds,  
441 *Physical chemistry chemical physics : PCCP*, 2015.

442 Charrier, J. G., and Anastasio, C.: Impacts of antioxidants on hydroxyl radical production from  
443 individual and mixed transition metals in a surrogate lung fluid, *Atmos. Environ.*, 45, 7555-7562,  
444 2011.

- 445 Charrier, J. G., McFall, A. S., Richards-Henderson, N. K., and Anastasio, C.: Hydrogen Peroxide  
446 Formation in a Surrogate Lung Fluid by Transition Metals and Quinones Present in Particulate Matter,  
447 Environ. Sci. Technol., 48, 7010-7017, 2014.
- 448 Chen, X., and Hopke, P. K.: A chamber study of secondary organic aerosol formation by limonene  
449 ozonolysis, Indoor Air, 20, 320-328, 2010.
- 450 Chen, X., Hopke, P. K., and Carter, W. P.: Secondary organic aerosol from ozonolysis of biogenic  
451 volatile organic compounds: chamber studies of particle and reactive oxygen species formation,  
452 Environ Sci Technol, 45, 276-282, 2011.
- 453 Cho, A. K., Sioutas, C., Miguel, A. H., Kumagai, Y., Schmitz, D. A., Singh, M., Eiguren-Fernandez,  
454 A., and Froines, J. R.: Redox activity of airborne particulate matter at different sites in the Los  
455 Angeles Basin, Environ. Res., 99, 40-47, 2005.
- 456 Crounse, J. D., Nielsen, L. B., Jørgensen, S., Kjaergaard, H. G., and Wennberg, P. O.: Autoxidation of  
457 organic compounds in the atmosphere, J. Phys. Chem. Lett., 4, 3513-3520, 2013.
- 458 Daumit, K. E., Carrasquillo, A. J., Sugrue, R. A., and Kroll, J. H.: Effects of Condensed-Phase  
459 Oxidants on Secondary Organic Aerosol Formation, J. Phys. Chem. A, 120, 1386-1394, 2016.
- 460 Dellinger, B., Pryor, W. A., Cueto, R., Squadrito, G. L., Hegde, V., and Deutsch, W. A.: Role of Free  
461 Radicals in the Toxicity of Airborne Fine Particulate Matter, Chemical Research in Toxicology, 14,  
462 1371-1377, 2001.
- 463 Dellinger, B., Loninicki, S., Khachatryan, L., Maskos, Z., Hall, R. W., Adoukpe, J., McFerrin, C.,  
464 and Truong, H.: Formation and stabilization of persistent free radicals, Proc. Combust. Inst., 31, 521-  
465 528, 2007.
- 466 Docherty, K. S., Wu, W., Lim, Y. B., and Ziemann, P. J.: Contributions of Organic Peroxides to  
467 Secondary Aerosol Formed from Reactions of Monoterpenes with O<sub>3</sub>, Environmental Science &  
468 Technology, 39, 4049-4059, 2005.
- 469 Dou, J., Lin, P., Kuang, B.-Y., and Yu, J. Z.: Reactive Oxygen Species Production Mediated by  
470 Humic-like Substances in Atmospheric Aerosols: Enhancement Effects by Pyridine, Imidazole, and  
471 Their Derivatives, Environ. Sci. Technol., 49, 6457-6465, 2015.
- 472 Ehn, M., Thornton, J. A., Kleist, E., Sipila, M., Junninen, H., Pullinen, I., Springer, M., Rubach, F.,  
473 Tillmann, R., Lee, B., Lopez-Hilfiker, F., Andres, S., Acir, I.-H., Rissanen, M., Jokinen, T.,  
474 Schobesberger, S., Kangasluoma, J., Kontkanen, J., Nieminen, T., Kurten, T., Nielsen, L. B.,  
475 Jørgensen, S., Kjaergaard, H. G., Canagaratna, M., Dal Maso, M., Berndt, T., Petaja, T., Wahner, A.,  
476 Kerminen, V.-M., Kulmala, M., Worsnop, D. R., Wildt, J., and Mentel, T. F.: A large source of low-  
477 volatility secondary organic aerosol, Nature, 506, 476-479, 2014.
- 478 Enami, S., Sakamoto, Y., and Colussi, A. J.: Fenton chemistry at aqueous interfaces, Proc. Natl. Acad.  
479 Sci. U.S.A., 111, 623-628, 2014.
- 480 Epstein, S. A., Blair, S. L., and Nizkorodov, S. A.: Direct photolysis of  $\alpha$ -pinene ozonolysis secondary  
481 organic aerosol: effect on particle mass and peroxide content, Environ. Sci. Technol., 48, 11251-  
482 11258, 2014.
- 483 Ervens, B.: Modeling the Processing of Aerosol and Trace Gases in Clouds and Fogs, Chem. Rev.,  
484 115, 4157-4198, 2015.

485 Fang, T., Verma, V., Bates, J. T., Abrams, J., Klein, M., Strickland, M. J., Sarnat, S. E., Chang, H. H.,  
486 Mulholland, J. A., Tolbert, P. E., Russell, A. G., and Weber, R. J.: Oxidative potential of ambient  
487 water-soluble PM<sub>2.5</sub> measured by Dithiothreitol (DTT) and Ascorbic Acid (AA) assays in the  
488 southeastern United States: contrasts in sources and health associations, *Atmos. Chem. Phys. Discuss.*,  
489 15, 30609-30644, 2015.

490 Fuller, S. J., Wragg, F. P. H., Nutter, J., and Kalberer, M.: Comparison of on-line and off-line  
491 methods to quantify reactive oxygen species (ROS) in atmospheric aerosols, *Atmos. Environ.*, 92, 97-  
492 103, 2014.

493 Gehling, W., and Dellinger, B.: Environmentally Persistent Free Radicals and Their Lifetimes in  
494 PM<sub>2.5</sub>, *Environ. Sci. Technol.*, 47, 8172-8178, 2013.

495 Gehling, W., Khachatryan, L., and Dellinger, B.: Hydroxyl radical generation from environmentally  
496 persistent free radicals (EPFRs) in PM<sub>2.5</sub>, *Environ Sci Technol*, 48, 4266-4272, 2014.

497 Gomes, L., Bergametti, G., Dulac, F., and Ezat, U.: Assessing the actual size distribution of  
498 atmospheric aerosols collected with a cascade impactor, *J. Aerosol Sci.*, 21, 47-59, 1990.

499 Gualtieri, M., Mantecca, P., Corvaja, V., Longhin, E., Perrone, M. G., Bolzacchini, E., and Camatini,  
500 M.: Winter fine particulate matter from Milan induces morphological and functional alterations in  
501 human pulmonary epithelial cells (A549), *Toxicology letters*, 188, 52-62, 2009.

502 Herrmann, H., Schaefer, T., Tilgner, A., Styler, S. A., Weller, C., Teich, M., and Otto, T.:  
503 Tropospheric Aqueous-Phase Chemistry: Kinetics, Mechanisms, and Its Coupling to a Changing Gas  
504 Phase, *Chem. Rev.*, 115, 4259-4334, 2015.

505 Huang, C. H., Ren, F. R., Shan, G. Q., Qin, H., Mao, L., and Zhu, B. Z.: Molecular mechanism of  
506 metal-independent decomposition of organic hydroperoxides by halogenated quinoid carcinogens and  
507 the potential biological implications, *Chem Res Toxicol*, 28, 831-837, 2015.

508 Hung, H.-F., and Wang, C.-S.: Experimental determination of reactive oxygen species in Taipei  
509 aerosols, *Journal of Aerosol Science*, 32, 1201-1211, 2001.

510 Jia, H., Nulaji, G., Gao, H., Wang, F., Zhu, Y., and Wang, C.: Formation and Stabilization of  
511 Environmentally Persistent Free Radicals Induced by the Interaction of Anthracene with Fe(III)-  
512 Modified Clays, *Environ. Sci. Technol.*, 2016.

513 Jimenez, J. L., Canagaratna, M. R., Donahue, N. M., Prevot, A. S. H., Zhang, Q., Kroll, J. H.,  
514 DeCarlo, P. F., Allan, J. D., Coe, H., Ng, N. L., Aiken, A. C., Docherty, K. S., Ulbrich, I. M.,  
515 Grieshop, A. P., Robinson, A. L., Duplissy, J., Smith, J. D., Wilson, K. R., Lanz, V. A., Hueglin, C.,  
516 Sun, Y. L., Tian, J., Laaksonen, A., Raatikainen, T., Rautiainen, J., Vaattovaara, P., Ehn, M., Kulmala,  
517 M., Tomlinson, J. M., Collins, D. R., Cubison, M. J., Dunlea, E. J., Huffman, J. A., Onasch, T. B.,  
518 Alfarra, M. R., Williams, P. I., Bower, K., Kondo, Y., Schneider, J., Drewnick, F., Borrmann, S.,  
519 Weimer, S., Demerjian, K., Salcedo, D., Cottrell, L., Griffin, R., Takami, A., Miyoshi, T.,  
520 Hatakeyama, S., Shimono, A., Sun, J. Y., Zhang, Y. M., Dzepina, K., Kimmel, J. R., Sueper, D.,  
521 Jayne, J. T., Herndon, S. C., Trimborn, A. M., Williams, L. R., Wood, E. C., Middlebrook, A. M.,  
522 Kolb, C. E., Baltensperger, U., and Worsnop, D. R.: Evolution of organic aerosols in the atmosphere,  
523 *Science*, 326, 1525-1529, 2009.

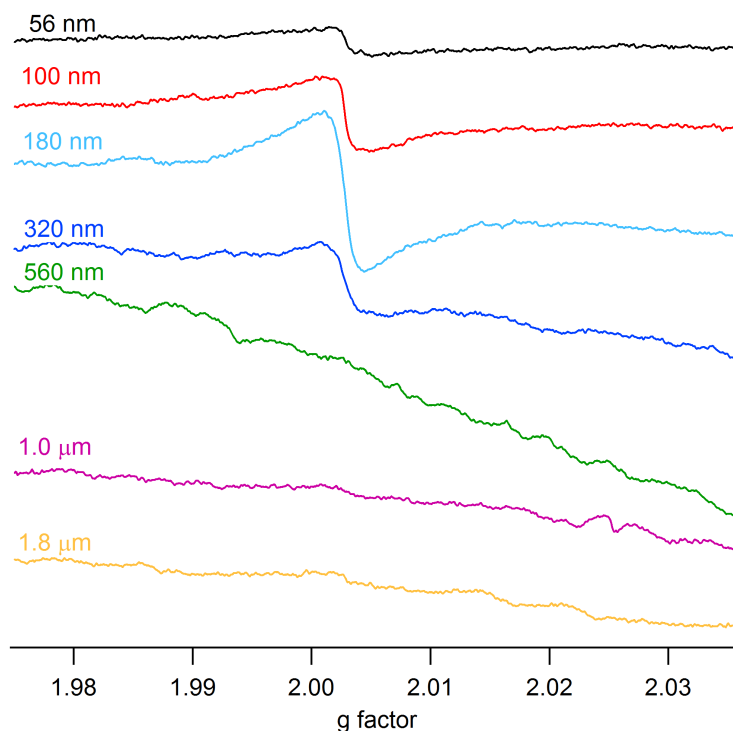
524 Kampf, C. J., Liu, F., Reinmuth-Selzle, K., Berkemeier, T., Meusel, H., Shiraiwa, M., and Poschl, U.:  
525 Protein Cross-Linking and Oligomerization through Dityrosine Formation upon Exposure to Ozone,  
526 *Environ Sci Technol*, 49, 10859-10866, 2015.

- 527 Khachatryan, L., and Dellinger, B.: Environmentally Persistent Free Radicals (EPFRs)-2. Are Free  
528 Hydroxyl Radicals Generated in Aqueous Solutions?, *Environ. Sci. Technol.*, 45, 9232-9239, 2011.
- 529 Khachatryan, L., Vejerano, E., Lomnicki, S., and Dellinger, B.: Environmentally Persistent Free  
530 Radicals (EPFRs). 1. Generation of Reactive Oxygen Species in Aqueous Solutions, *Environ. Sci.*  
531 *Technol.*, 45, 8559-8566, 2011.
- 532 Kumagai, Y., Arimoto, T., Shinyashiki, M., Shimojo, N., Nakai, Y., Yoshikawa, T., and Sagai, M.:  
533 Generation of reactive oxygen species during interaction of diesel exhaust particle components with  
534 NADPH-cytochrome P450 reductase and involvement of the bioactivation in the DNA damage, *Free*  
535 *Radical Biol. Med.*, 22, 479-487, 1997.
- 536 Lakey, P. S. J., Berkemeier, T., Tong, H., Arangio, A. M., Lucas, K., Pöschl, U., and Shiraiwa, M.:  
537 Chemical exposure-response relationship between air pollutants and reactive oxygen species in the  
538 human respiratory tract, *Sci. Rep.*, 6, 32916, 2016.
- 539 Lelieveld, J., Evans, J. S., Fnais, M., Giannadaki, D., and Pozzer, A.: The contribution of outdoor air  
540 pollution sources to premature mortality on a global scale, *Nature*, 525, 367-371, 2015.
- 541 Lim, Y. B., Tan, Y., Perri, M. J., Seitzinger, S. P., and Turpin, B. J.: Aqueous chemistry and its role in  
542 secondary organic aerosol (SOA) formation, *Atmos. Chem. Phys.*, 10, 10521-10539, 2010.
- 543 Lin, P., and Yu, J. Z.: Generation of Reactive Oxygen Species Mediated by Humic-like Substances in  
544 Atmospheric Aerosols, *Environ. Sci. Technol.*, 45, 10362-10368, 2011.
- 545 Lucas, K., and Maes, M.: Role of the Toll Like Receptor (TLR) Radical Cycle in Chronic  
546 Inflammation: Possible Treatments Targeting the TLR4 Pathway, *Mol. Neurobiol.*, 48, 190-204, 2013.
- 547 McNeill, V. F., Woo, J. L., Kim, D. D., Schwier, A. N., Wannell, N. J., Sumner, A. J., and Barakat, J.  
548 M.: Aqueous-phase secondary organic aerosol and organosulfate formation in atmospheric aerosols:  
549 A modeling study, *Environ. Sci. Technol.*, 46, 8075-8081, 2012.
- 550 McWhinney, R. D., Zhou, S., and Abbatt, J. P. D.: Naphthalene SOA: redox activity and  
551 naphthoquinone gas-particle partitioning, *Atmos. Chem. Phys.*, 13, 9731-9744, 2013.
- 552 Nel, A.: Air pollution-related illness: Effects of particles, *Science*, 308, 804-806, 2005.
- 553 Ouari, O., Hardy, M., Karoui, H., and Tordo, P.: Recent developments and applications of the coupled  
554 EPR/Spin trapping technique (EPR/ST), in: *Electron Paramagnetic Resonance: Volume 22*, The Royal  
555 Society of Chemistry, 1-40, 2011.
- 556 Pavlovic, J., and Hopke, P. K.: Detection of radical species formed by the ozonolysis of  $\alpha$ -pinene,  
557 *Journal of Atmospheric Chemistry*, 66, 137-155, 2011.
- 558 Pöhlker, C., Wiedemann, K. T., Sinha, B., Shiraiwa, M., Gunthe, S. S., Smith, M., Su, H., Artaxo, P.,  
559 Chen, Q., Cheng, Y., Elbert, W., Gilles, M. K., Kilcoyne, A. L. D., Moffet, R. C., Weigand, M.,  
560 Martin, S. T., Pöschl, U., and Andreae, M. O.: Biogenic potassium salt particles as seeds for  
561 secondary organic aerosol in the Amazon, *Science*, 337, 1075-1078, 2012.
- 562 Pope, C. A., and Dockery, D. W.: Health effects of fine particulate air pollution: lines that connect, *J.*  
563 *Air Waste Manag. Assoc.*, 56, 709-742, 2006.
- 564 Pöschl, U., and Shiraiwa, M.: Multiphase Chemistry at the Atmosphere-Biosphere Interface  
565 Influencing Climate and Public Health in the Anthropocene, *Chem. Rev.*, 115, 4440-4475, 2015.

- 566 Pryor, W. A., Squadrito, G. L., and Friedman, M.: The cascade mechanism to explain ozone toxicity -  
567 The role of lipid ozonation products, *Free Radical Biol. Med.*, 19, 935-941, 1995.
- 568 Reinmuth-Selzle, K., Ackaert, C., Kampf, C. J., Samonig, M., Shiraiwa, M., Kofler, S., Yang, H.,  
569 Gadermaier, G., Brandstetter, H., Huber, C. G., Duschl, A., Oostingh, G. J., and Pöschl, U.: Nitration  
570 of the birch pollen allergen Bet v 1.0101: Efficiency and site-selectivity of liquid and gaseous  
571 nitrating agents, *J. Proteome Res.*, 13, 1570–1577, 2014.
- 572 Saffari, A., Daher, N., Shafer, M. M., Schauer, J. J., and Sioutas, C.: Seasonal and spatial variation in  
573 reactive oxygen species activity of quasi-ultrafine particles (PM<sub>0.25</sub>) in the Los Angeles metropolitan  
574 area and its association with chemical composition, *Atmos. Environ.*, 79, 566-575, 2013.
- 575 Saffari, A., Daher, N., Shafer, M. M., Schauer, J. J., and Sioutas, C.: Global perspective on the  
576 oxidative potential of airborne particulate matter: a synthesis of research findings, *Environ Sci  
577 Technol*, 48, 7576-7583, 2014.
- 578 Sanchez-Cruz, P., Santos, A., Diaz, S., and Alegria, A. E.: Metal-independent reduction of hydrogen  
579 peroxide by semiquinones, *Chem Res Toxicol*, 27, 1380-1386, 2014.
- 580 Shaltout, A. A., Boman, J., Shehadeh, Z. F., Al-Malawi, D.-a. R., Hemed, O. M., and Morsy, M. M.:  
581 Spectroscopic investigation of PM<sub>2.5</sub> collected at industrial, residential and traffic sites in Taif, Saudi  
582 Arabia, *Journal of Aerosol Science*, 79, 97-108, 2015.
- 583 Shiraiwa, M., Sosedova, Y., Rouviere, A., Yang, H., Zhang, Y., Abbatt, J. P. D., Ammann, M., and  
584 Pöschl, U.: The role of long-lived reactive oxygen intermediates in the reaction of ozone with aerosol  
585 particles, *Nature Chem.*, 3, 291-295, 2011.
- 586 Shiraiwa, M., Selzle, K., Yang, H., Sosedova, Y., Ammann, M., and Pöschl, U.: Multiphase chemical  
587 kinetics of the nitration of aerosolized protein by ozone and nitrogen dioxide, *Environ Sci Technol*, 46,  
588 6672-6680, 2012.
- 589 Shiraiwa, M., Berkemeier, T., Schilling-Fahnestock, K. A., Seinfeld, J. H., and Pöschl, U.: Molecular  
590 corridors and kinetic regimes in the multiphase chemical evolution of secondary organic aerosol,  
591 *Atmos. Chem. Phys.*, 14, 8323-8341, 2014.
- 592 Squadrito, G. L., Cueto, R., Dellinger, B., and Pryor, W. A.: Quinoid redox cycling as a mechanism  
593 for sustained free radical generation by inhaled airborne particulate matter, *Free Radical Biol. Med.*,  
594 31, 1132-1138, 2001.
- 595 Stoll, S., and Schweiger, A.: EasySpin, a comprehensive software package for spectral simulation and  
596 analysis in EPR, *Journal of magnetic resonance*, 178, 42-55, 2006.
- 597 Strak, M., Janssen, N. A., Godri, K. J., Gosens, I., Mudway, I. S., Cassee, F. R., Lebret, E., Kelly, F.  
598 J., Harrison, R. M., Brunekreef, B., Steenhof, M., and Hoek, G.: Respiratory health effects of airborne  
599 particulate matter: the role of particle size, composition, and oxidative potential-the RAPTES project,  
600 *Environmental health perspectives*, 120, 1183-1189, 2012.
- 601 Sueishi, Y., Kamogawa, E., Nakamura, H., Ukai, M., Kunieda, M., Okada, T., Shimmei, M., and  
602 Kotake, Y.: Kinetic Evaluation of Spin Trapping Rate Constants of New CYPMPO-type Spin Traps  
603 for Superoxide and Other Free Radicals, *Z. Phys. Chem.*, 229, 317-326, 2015.
- 604 Tong, H., Arangio, A. M., Lakey, P. S. J., Berkemeier, T., Liu, F., Kampf, C. J., Brune, W. H., Pöschl,  
605 U., and Shiraiwa, M.: Hydroxyl radicals from secondary organic aerosol decomposition in water,  
606 *Atmos. Chem. Phys.*, 16, 1761-1771, 2016.

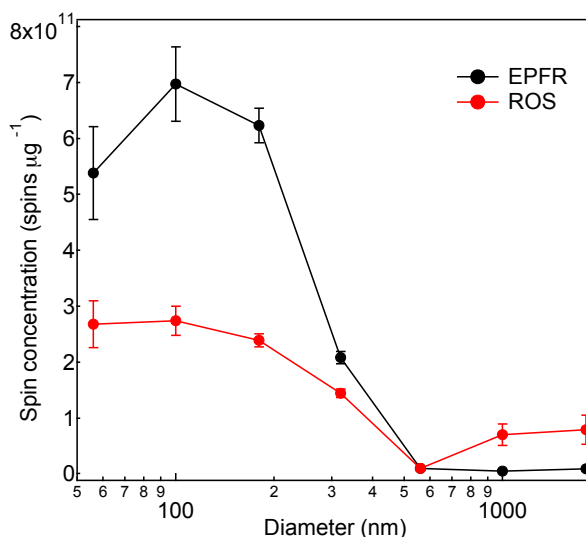
- 607 Truong, H., Lomnicki, S., and Dellinger, B.: Potential for Misidentification of Environmentally  
608 Persistent Free Radicals as Molecular Pollutants in Particulate Matter, *Environ. Sci. Technol.*, 44,  
609 1933-1939, 2010.
- 610 Vejerano, E., Lomnicki, S., and Dellinger, B.: Formation and stabilization of combustion-generated  
611 environmentally persistent free radicals on an Fe(III)2O3/silica surface, *Environ Sci Technol*, 45, 589-  
612 594, 2011.
- 613 Venkatachari, P., Hopke, P. K., Grover, B. D., and Eatough, D. J.: Measurement of Particle-Bound  
614 Reactive Oxygen Species in Rubidoux Aerosols, *Journal of Atmospheric Chemistry*, 50, 49-58, 2005.
- 615 Venkatachari, P., Hopke, P. K., Brune, W. H., Ren, X., Leshner, R., Mao, J., and Mitchell, M.:  
616 Characterization of Wintertime Reactive Oxygen Species Concentrations in Flushing, New York,  
617 *Aerosol Science and Technology*, 41, 97-111, 2007.
- 618 Verma, V., Fang, T., Xu, L., Peltier, R. E., Russell, A. G., Ng, N. L., and Weber, R. J.: Organic  
619 Aerosols Associated with the Generation of Reactive Oxygen Species (ROS) by Water-Soluble  
620 PM2.5, *Environ. Sci. Technol.*, 49, 4646-4656, 2015a.
- 621 Verma, V., Fang, T., Xu, L., Peltier, R. E., Russell, A. G., Ng, N. L., and Weber, R. J.: Organic  
622 aerosols associated with the generation of reactive oxygen species (ROS) by water-soluble PM2.5,  
623 *Environmental science & technology*, 49, 4646-4656, 2015b.
- 624 Verma, V., Wang, Y., El-Affifi, R., Fang, T., Rowland, J., Russell, A. G., and Weber, R. J.:  
625 Fractionating ambient humic-like substances (HULIS) for their reactive oxygen species activity –  
626 Assessing the importance of quinones and atmospheric aging, *Atmos. Environ.*, 120, 351-359, 2015c.
- 627 Wang, D., Pakbin, P., Shafer, M. M., Antkiewicz, D., Schauer, J. J., and Sioutas, C.: Macrophage  
628 reactive oxygen species activity of water-soluble and water-insoluble fractions of ambient coarse,  
629 PM2.5 and ultrafine particulate matter (PM) in Los Angeles, *Atmos. Environ.*, 77, 301-310, 2013.
- 630 Wang, Y., Kim, H., and Paulson, S. E.: Hydrogen peroxide generation from alpha- and beta-pinene  
631 and toluene secondary organic aerosols, *Atmos. Environ.*, 45, 3149-3156, 2011.
- 632 Wang, Y., Arellanes, C., and Paulson, S. E.: Hydrogen Peroxide Associated with Ambient Fine-Mode,  
633 Diesel, and Biodiesel Aerosol Particles in Southern California, *Aerosol Sci. Technol.*, 46, 394-402,  
634 2012.
- 635 West, J. J., Cohen, A., Dentener, F., Brunekreef, B., Zhu, T., Armstrong, B., Bell, M. L., Brauer, M.,  
636 Carmichael, G., Costa, D. L., Dockery, D. W., Kleeman, M., Krzyzanowski, M., Künzli, N., Liousse,  
637 C., Lung, S.-C. C., Martin, R. V., Pöschl, U., Pope, C. A., Roberts, J. M., Russell, A. G., and  
638 Wiedinmyer, C.: “What We Breathe Impacts Our Health: Improving Understanding of the Link  
639 between Air Pollution and Health”, *Environ. Sci. Technol.*, 50, 4895-4904, 2016.
- 640 Winterbourn, C. C.: Reconciling the chemistry and biology of reactive oxygen species, *Nature Chem.*  
641 *Biol.*, 4, 278-286, 2008.
- 642 Zhao, H., Joseph, J., Zhang, H., Karoui, H., and Kalyanaraman, B.: Synthesis and biochemical  
643 applications of a solid cyclic nitron spin trap: a relatively superior trap for detecting superoxide  
644 anions and glutathyl radicals, *Free Radical Biol. Med.*, 31, 599-606, 2001.
- 645 Zhu, B. Z., Kalyanaraman, B., and Jiang, G. B.: Molecular mechanism for metal-independent  
646 production of hydroxyl radicals by hydrogen peroxide and halogenated quinones, *Proc Natl Acad Sci*  
647 *U S A*, 104, 17575-17578, 2007a.

- 648 Zhu, B. Z., Zhao, H. T., Kalyanaraman, B., Liu, J., Shan, G. Q., Du, Y. G., and Frei, B.: Mechanism  
649 of metal-independent decomposition of organic hydroperoxides and formation of alkoxy radicals by  
650 halogenated quinones, *Proc Natl Acad Sci U S A*, 104, 3698-3702, 2007b.
- 651 Zhu, B. Z., Shan, G. Q., Huang, C. H., Kalyanaraman, B., Mao, L., and Du, Y. G.: Metal-independent  
652 decomposition of hydroperoxides by halogenated quinones: detection and identification of a quinone  
653 ketoxy radical, *Proc Natl Acad Sci U S A*, 106, 11466-11471, 2009.
- 654 Ziemann, P. J., and Atkinson, R.: Kinetics, products, and mechanisms of secondary organic aerosol  
655 formation, *Chem. Soc. Rev.*, 41, 6582-6605, 2012.
- 656
- 657
- 658



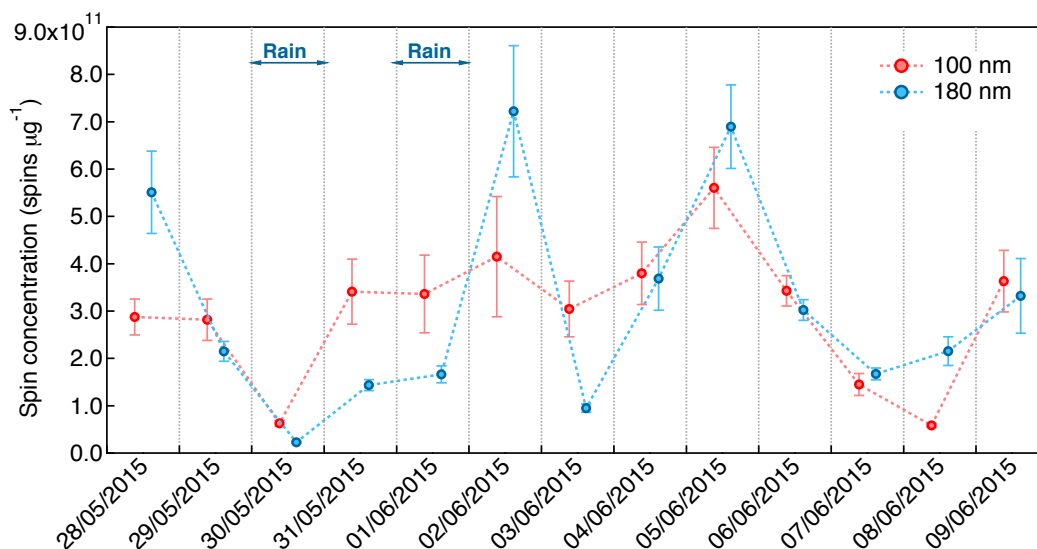
659  
 660 **Figure 1:** Electron paramagnetic resonance (EPR) spectra of atmospheric aerosol impactor  
 661 samples with lower cut-off diameters in the range of 56 nm to 1.8 micrometer collected in  
 662 Mainz, Germany during 26 - 27 June, 2015.

663



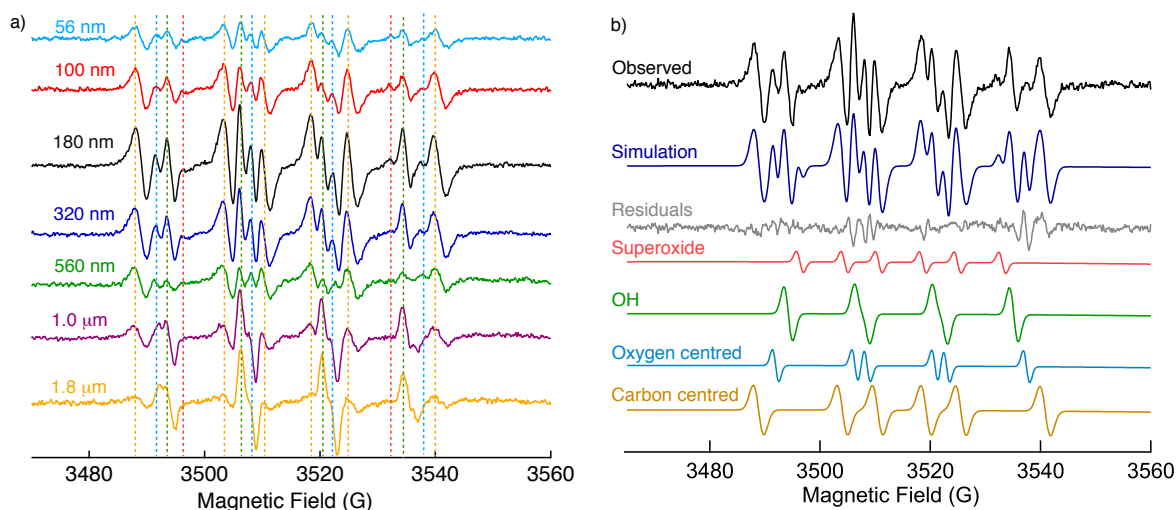
664  
 665 **Figure 2:** Concentrations (spins per microgram of particles) of environmentally persistent  
 666 free radicals (EPFR) and radical forms of reactive oxygen species (ROS) in atmospheric  
 667 aerosol samples plotted against particle diameter. The error bars represent standard errors  
 668 based on uncertainties of the particle mass and signal integration of EPR spectra.

669



670  
671  
672  
673  
674  
675  
676  
677

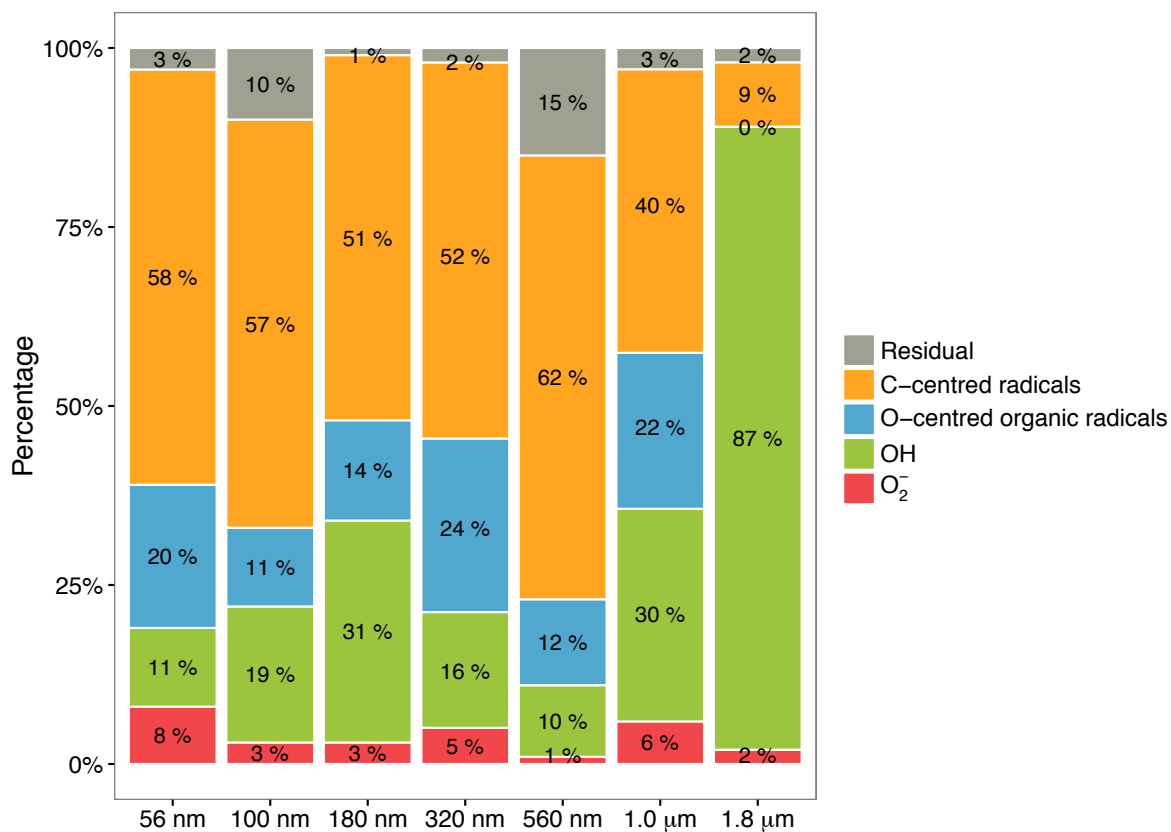
**Figure 3:** Temporal evolution of concentrations of environmentally persistent free radicals (EPFR) contained in atmospheric aerosol samples with lower cutoff diameters of 100 nm (red) and 180 nm (blue), measured in Mainz, Germany during May – June 2015. The error bars represent standard errors based on uncertainties of the particle mass and signal integration of EPR spectra.



678

679 **Figure 4:** a) Electron paramagnetic resonance (EPR) spectra of ambient aerosol impactor  
 680 samples (Mainz, Germany, 26-27 June 2015) with lower cut-off diameters in the range of 56  
 681 nm to 1.8 μm extracted in water mixed with the spin-trapping agent BMPO. Dashed lines  
 682 indicate the position of each peak for different types of trapped radicals of  $O_2^-$  (red), OH  
 683 (green), carbon-centred (orange), and oxygen-centred organic radicals (light blue). b)  
 684 Simulation of the EPR spectrum of the atmospheric aerosol impactor sample with particle  
 685 diameters in the range of 180-320 nm (lower to upper cut-off) by deconvoluting into  $O_2^-$ , OH,  
 686 O-centred and C-centred organic radicals (Blue = synthesis, grey = residual).

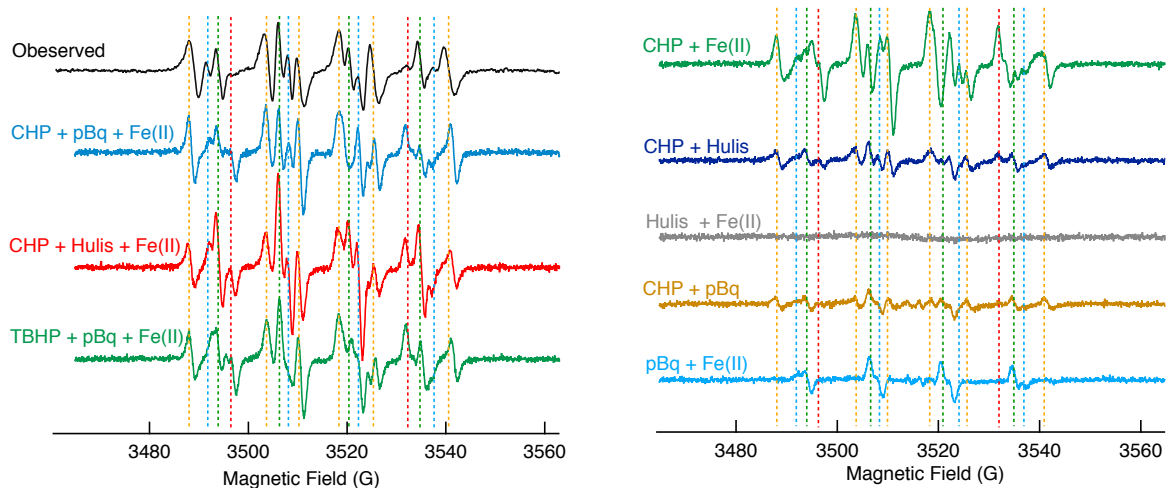
687



688

689 **Figure 5:** Relative amount of ROS in atmospheric aerosol impactor samples with lower cut-  
 690 off diameters in the range of 50 nm -1.8 μm (Mainz, Germany, 26-27 June 2015): O<sub>2</sub><sup>-</sup> (red),  
 691 OH (green), carbon-centred (orange), oxygen-centred organic radicals (blue) and residual  
 692 (unidentified, grey).

693

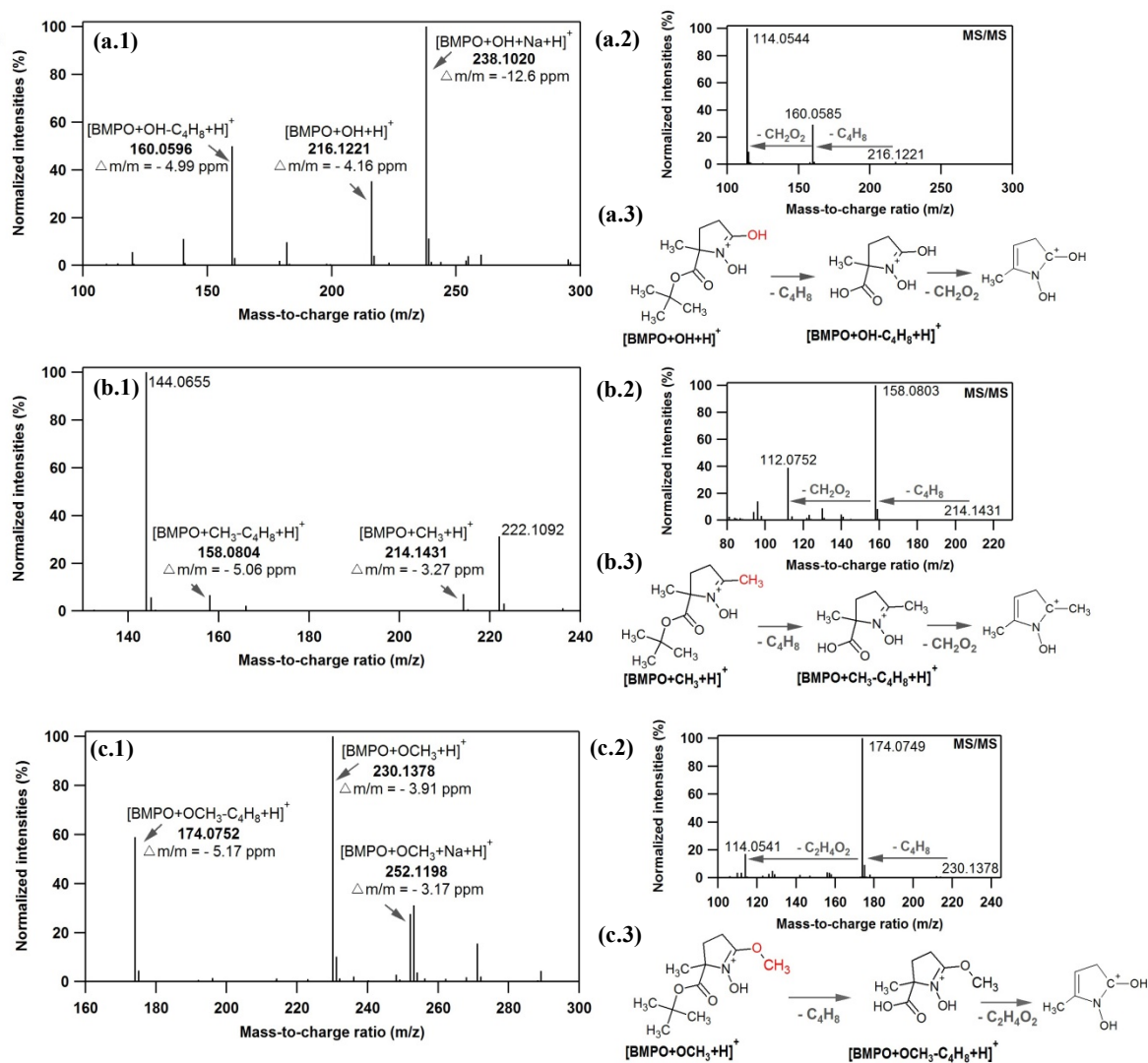


694

695 **Figure 6:** Electron paramagnetic resonance (EPR) spectra of atmospheric aerosol impactor  
 696 sample with particle diameters in the range of 180-320 nm (lower to upper cut-off) extracted  
 697 with water and BMPO (black) and of aqueous substance mixtures with the following  
 698 ingredients: cumene hydroperoxide (CHP), p-benzoquinone (pBq) and Fe(II) (light blue), t-  
 699 butyl hydroperoxide (TBHP). The dashed vertical lines indicate the main peaks of BMPO  
 700 adducts with  $O_2^-$  (red), OH (green), carbon- (light blue), and oxygen-centred organic  
 701 radicals (light blue).

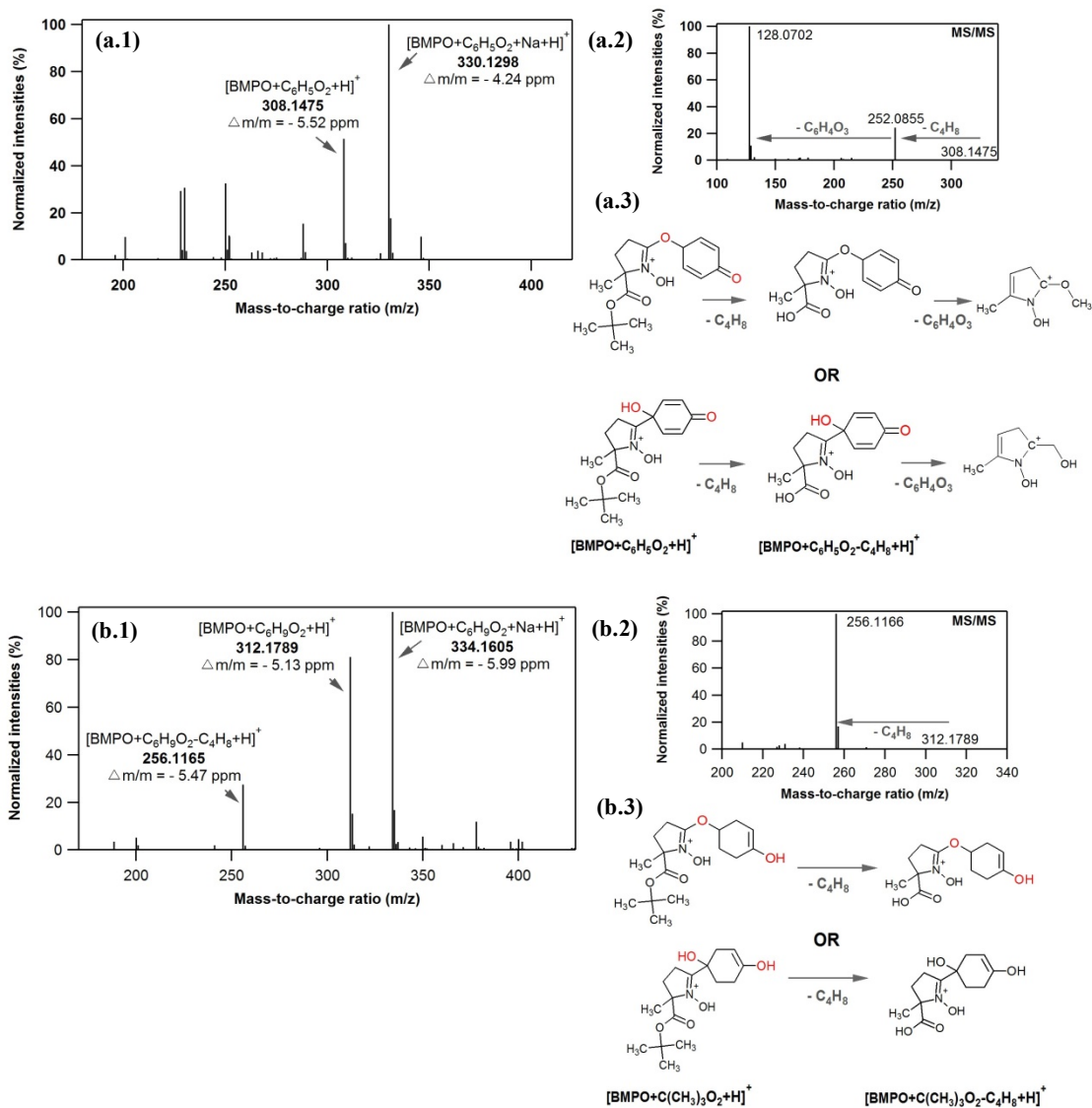


**Figure A1:** EPR spectra of atmospheric aerosol impactor samples with lower cut-off diameters of 56 nm (black), 100 nm (red), 180 nm (light blue) and 320 nm (green) for the measurement period during 28 May – 9 June 2015.



712

713 **Figure A2:** Mass spectra obtained with LC-MS/MS in the positive ionization mode from the  
 714 mixture of tert-butyl hydroperoxide, p-benzoquinone and BMPO in the presence of iron  
 715 (solution (1)). MS spectra of **(a.1)** BMPO+OH, **(b.1)** BMPO+CH<sub>3</sub> and **(c.1)** BMPO+OCH<sub>3</sub>.  
 716 MS/MS spectra of **(a.2)** BMPO+OH, **(b.2)** BMPO+CH<sub>3</sub>, and **(c.2)** BMPO+OCH<sub>3</sub>. Proposed  
 717 fragmentation pathways of **(a.3)** BMPO+OH, **(b.3)** BMPO+CH<sub>3</sub> and **(c.3)** BMPO+OCH<sub>3</sub>.



718

719 **Figure A3:** Mass spectra obtained with LC-MS/MS in the positive ionization mode for  
 720 solution (1). MS spectra of **(a.1)**  $\text{BMPO}+\text{C}_6\text{H}_5\text{O}_2$  and **(b.1)**  $\text{BMPO}+\text{C}_6\text{H}_9\text{O}_2$ . MS/MS spectra  
 721 of **(a.2)**  $\text{BMPO}+\text{C}_6\text{H}_5\text{O}_2$  and **(b.2)**  $\text{BMPO}+\text{C}_6\text{H}_9\text{O}_2$ . Proposed fragmentation pathway of **(a.3)**  
 722  $\text{BMPO}+\text{C}_6\text{H}_5\text{O}_2$  and **(b.3)**  $\text{BMPO}+\text{C}_6\text{H}_9\text{O}_2$ .

723